FREQUENCY DOMAIN CHANNEL ESTIMATION AND SYMBOL DETECTION FOR IMPULSE RADIO ULTRA-WIDEBAND SYSTEMS WITH SHORT CYCLIC PREFIX

by

Salim Bahçeci

B. S., Electrical and Electronics Engineering, Gaziantep University, 2006

Submitted to the Institute for Graduate Studies in
Science and Engineering in partial fulfillment of
the requirements for the degree of
Master of Science

Graduate Program in Electrical and Electronics Engineering
Boğaziçi University

2009

ACKNOWLEDGEMENTS

I would like to to express my gratitude to Assist. Prof. Mutlu Koca for his guidance and help during the preparation of this thesis. His valuable ideas, suggestions and comments make this thesis possible.

I am thankful to the members of the committee, namely, Prof. Emin Anarım and Prof. Cem Ersoy.

I would like to thank to the members of Wireless Communication Laboratory who always supported me to carry on when I stuck at dead-end.

I am grateful to my family for their supports. They always supported me whatever the conditions were. Without their supports it would be impossible for me to come at that point. They always supported me and I am sure they will support me in the future.

This thesis has been supported by TUBiTAK EEEAG under the grants 105E077

ABSTRACT

FREQUENCY DOMAIN CHANNEL ESTIMATION AND SYMBOL DETECTION FOR IMPULSE RADIO ULTRA-WIDEBAND SYSTEMS WITH SHORT CYCLIC PREFIX

Frequency Domain (FD) reception techniques provide the telecommunication system designers with low complexity receiver structures. However, when ultra-wideband (UWB) communication is considered with long channel impulse responses adding cyclic prefix (CP) causes decrease in system bandwidth efficiency. Using short cyclic prefix to compensate for bandwidth efficiency lost causes performance lost in terms of bit error rate (BER). In this thesis, we consider iterative cancellation of inter block interference (IBI) caused by short CP usage in impulse radio ultra-wideband (IR-UWB) communication. Pilot blocks aided FD recursive least squares (RLS) channel estimation is considered and an iterative algorithm is proposed for the IBI error cancellation. In addition, for the detection of the transmitted information data blocks a receiver structure is proposed composed of soft input soft output frequency domain minimum mean square error (SISO FD MMSE) equalizer, SISO repetition decoder and IBI estimation block operating in turbo manner.

ÖZET

KISA ÇEVRİMSEL ÖN EK KULLANILAN DÜRTÜ RADYO ULTRA-GENİŞBANT SİSTEMLER İÇİN FREKANS TANIM KÜMESİNDE KANAL KESTİRİMİ VE SEMBOL ALGILAMASI

Frekans tanım kümesi (FTK) algılama teknikleri telekomünikasyon sistem tasarımcılarına az karmaşık algılayıcı yapıları sağlar. Ancak uzun kanal dürtü tepkili ultra geniş bant haberleşme düşünüldüğünde çevrimsel ön ek eklemek sistemin bantgenişliği etkinliğinin azalmasına neden olur. Bantgenişliği etkinliğinin azalmasını telafi etmek için kısa çevrimsel ön ek kullanımı bit hata oranına (BHO) göre başarım kaybına neden olur. Bu tezde dürtü radyo ultra geniş bant haberleşmede kısa çevrimsel ön ek kullanılmasından dolayı oluşan bloklar arası girişimin (BAG) özyineli olarak ortadan kaldırılmasını ele aldık. Öncü blok yardımlı FTK özyineli en küçük kareler (ÖEKK) kanal kestirimi ele alındı ve BAG'ı özyineli olarak ortadan kaldıran bir algoritma önerildi. Ek olarak, iletilen bilgi veri bloklarının algılamasında turbo şeklinde çalışan yumuşak girdi yumuşak çıktı frekans tanım kümesi en küçük ortalama kareler hatası denkleştirici, yumuşak girdi yumuşak çıktı tekrar kodçözücü ve BAG kestirim bloğundan oluşan bir alglayıcı yapısı önerildi.

TABLE OF CONTENTS

LIST OF FIGURES

LIST OF TABLES

LIST OF SYMBOLS/ABBREVIATIONS

$*$	Linear convolution
$\lfloor . \rfloor$	Integer floor operation
$< . >_{N_b N_f}$	Modulo operation with respect to $N_b N_f$
$()^H$	Hermitian operator
$Cov(x, y)$	Covariance of x and y
$E(.)$	Expectation operator
$\Pi(.)$	Interleaving operator
$\Pi^{-1}(.)$	Deinterleaving operator
$a^n(i)$	Energy coefficient for the ith received sample in nth block
$\mathbf{b^n}$	Vector collecting nth data bits
$d(i)^{n-1}$	ith chip value of the (n-1)th data block
$\mathbf{d'^n}$	Vector collecting data bits after spreading
$\mathbf{d^n}$	Vector collecting data bits after spreading and interleaving
$\mathbf{d^n}$	Vector collecting transmitted chip values
$\bar{d}(i)$	Expected value of the ith chip position
$\hat{d}(i)$	Estimated value of the ith chip position
$\bar{\mathbf{d}}(i)$	Vector collecting the expected value of the chip positions
$\hat{\mathbf{d}}(i)$	Vector collecting the estimated value of the chip positions
$\mathbf{D}_C^n$	Circular matrix collecting chip values of the nth block
$\mathbf{D}^n$	Vector collecting chip values of nth block in frequency domain
$\hat{e}^n(i)$	IBI error estimate for the ith received sample in nth block
$e(i)^n$	ith IBI error term for the nth block
$\mathbf{e}^n$	Vector collecting IBI errors of nth block
$\mathbf{E}^n$	Vector collecting IBI errors of nth block in frequency domain
$\hat{\mathbf{E}}^n$	Vector collecting the estimates of IBI errors of nth block in frequency domain
f_c	Band center frequency
$\mathbf{F}$	Discrete Fourier transform matrix
$F_{l,k}$	(l,k)th entry of discrete fourier transform matrix

$h(l)$	Path gain of lth path
$h(t)$	Channel impulse response
$\mathbf{h}$	Vector collecting the channel impulse responses
$\mathbf{H}_C$	Circular matrix collecting channel coefficients
$\hat{\mathbf{H}}^n$	Vector collecting estimate of the channel impulse response for the nth received block in frequency domain
$\mathbf{H}$	Vector collecting the channel impulse response in frequency domain
L	Path number of channel impulse response
$L_{in}^E d(i)$	Log likelihood ratio of ith chip position at the input of the equalizer
$L_{out}^E d(i)$	Log likelihood ratio of ith chip position at the output of the equalizer
$L_{in}^D d'(i)$	Log likelihood ratio of ith chip position after deinterleaving at the input of the decoder
$L_{out}^D d'(i)$	Extrinsic log likelihood ratio of ith chip position after deinterleaving at the output of the decoder
$\mathbf{M}^n$	Diagonal matrix collecting fourier transforms of nth data block
M_k^n	kth bin of the nth data block after fourier transform
N_b	Number of bits in a data block
N_f	Number of frames per symbol
N_k	Number of chips added as cyclic prefix
$N_0/2$	Variance of additive white gaussian noise
$r(m)^n$	mth received sample of the nth block before the cyclic prefix extraction
$r(i)^n$	ith received sample of the nth block after the cyclic prefix extraction
$\mathbf{r^n}$	Vector collecting received samples after CP removal
$\mathbf{R}^n$	Vector collecting samples of nth received block in frequency domain
$s(t)^n$	Transmitted signal for nth block
T_f	Frame duration
T_s	Symbol duration

T_p	Pulse duration
$\tau(l)$	Path delay of the lth path
$w(m)$	mth sample of taken from AWGN process before the cyclic prefix extraction
$w(i)$	ith sample of taken from AWGN process after the cyclic prefix extraction
σ_w^2	Variance of additive white gaussian noise
$\mathbf{w}$	Vector collecting AWGN samples
$\mathbf{W}$	Vector collecting AWGN samples in frequency domain
Ψ	Diagonal matrix collecting Fourier transforms of channel impulse responses
ψ_k	kth bin of the channel impulse response after fourier transform
$\{\Lambda_{out}^D b(i)\}$	A posteriori log likelihood ratio of ith data bit at the output of the decoder
$\mathbf{\Lambda}$	Vector collecting the channel impulse response in frequency domain
$\hat{\sigma}^2$	Variance of the chip estimation error
μ	Mean of the chip estimation error
BER	Bit Error Rate
BFSK	Binary Phase Shift Keying
CIR	Channel Impulse Response
CP	Cyclic Prefix
DS-SS	Direct Sequence Spread Spectrum
FD	Frequency Domain
FDE	Frequency Domain Equalizer
FFT	Fast Fourier Transform
GPS	Global Positioning System
IFFT	Inverse Fast Fourier Transform
ISI	Inter Symbol Interference
IR	Impulse Radio
IBI	Inter Block Interference
LE	Linear Equalizer
ML	Maximum-Likelihood

MAP	Maximum a Posteriori Probability
MC	Multi-Carrier
MMSE	Minimum Mean Square Error
NLOS	Non-Line-of-Sigth
NMSE	Normalized Mean Square Error
OFDM	Orthogonal Frequency-Division Multiplexing
PPM	Pulse Position Modulation
PAM	Pulse Amplitude Modulation
RLS	Recursive Least Square
SNR	Signal-to-Noise Ratio
SC	Single-Carrier
SISO	Soft Input Soft Output
SS	Spread Spectrum
TH-SS	Time Hopping Spread Spectrum
US	United States
UWB	Ultra-Wideband
W	Transmission bandwidth
WLAN	Wireless Local Area Network
QPSK	Quadrature Phase Shift Keying
ZF	Zero Forcing

1. INTRODUCTION

Communication systems have always had an important place in humans lives. In past, people were communicating with different means such as sound, light. In 19. century with the invention of the electricity people have begun to use electrical signals for communication purposes. People generated electrical signals for communication purpose and transmitted them through wires. Today, we still use wires for communication but we also developed other means of communication.

With the invention of the electromagnetic waves, we began to use these waves to transmit electrical signal from one place to another. By doing so we get rid of the necessity of using long wires to communicate. However, this new technology also brought some disadvantages. In wireless communication, we use air as a communication medium. In this medium transmitted signals encounter severe attenuation as well as reflection, scattering and shadowing. These phenomena cause the transmitted signals to interact with each other. These interactions result with the constructive or destructive superposition of the transmitted signals. Due to constructive and destructive superposition of the transmitted signals it becomes infeasible to detect signal correctly.

To overcome these problems we can developed new modulation techniques also we can design new transmitter or receiver structures. Usually these new receivers are more complex than the wired communication system receivers, its because of the phenomena mentioned above. Researcher are trying to develop new receiver structures such that it can detect the transmitted signal as correctly as possible while it has low complexity.

For a typical wireless communication system it is expected to have a low bit error rate (BER) probability for a small signal-to-noise ratio (SNR). Besides on these it is also expected to have low complexity transmitters and receivers. Usually there is a trade-off between these three. If you want to have low BER probability with small SNR you can use some channel codding or error control codding algorithms. But this

comes with a cost, to implement coding on the transmitter and decoding on the receiver you need to use more components causing increase in complexity. Or you may need to perform more steps to estimate a received signal. If you keep same complexity level you will need more times to estimate a received signal that will be a problem for a real time communication.

Different than wired communication, in wireless communication we have extra difficulties. As it is previously stated reflection, scattering and shadowing cause a phenomenon called multipath effect [1]. The presence of multipath effect causes severe limitations on the receiver performance. So in wireless communication to obtain good performances we need to take some measures against the multipath effect. These extra measurements causes increase in complexity.

1.1. Background and Related Work

Multipath effect causes a time delay dispersion and there is a dual relation between time delay dispersion and frequency selectivity, i.e., the greater the time dispersion, the greater the frequency selectivity of the channel response. If we have a hostile communication medium that has a very long multipath delay spread then we have a frequency selective channel. To combat with this kind of frequency selective channels and other impairments caused by hostile transmission medium some different transmission and modulation techniques can be used such as multi-carrier (MC) and single-carrier (SC) transmission techniques [2].

MC modulation schemes are know to be very robust against severe time dispersion effect of multi path propagation, without requiring complex receiver implementations. On the other hand conventional single carrier modulation schemes have very high receiver complexity, mostly because of the time domain equalizers they use.

Following we give some information about both kind of modulation schemes, problems they face and some solutions proposed for these problems. Also we give information about UWB systems, their problems they face similar with conventional

communication systems and some researches made to overcome these problems.

1.1.1. OFDM Systems

Orthogonal frequency-division multiplexing (OFDM) is an efficient MC transmission technique [3]. OFDM transmits multiple modulated subscribers in parallel. Each of these subscribers uses a small portion of the assigned available bandwidth. Since channel effects only the amplitude and phase of each subscriber, compensation for frequency selective fading is done by equalizing each subscriber's gain and phase.

To generate subscribers, inverse fast Fourier transform (IFFT) is performed at the transmitter on blocks of M data symbols. Extraction on the subscribers at the receiver is done by performing the fast Fourier transform (FFT) operation on blocks of M symbols. In order to make the received block to appear to be periodic with period M and to prevent contamination of a block by inter block interference (IBI) from the previous blocks, a cyclic prefix (CP) whose length in data symbols exceeds the maximum expected delay spread is added to the beginning of each block. The cyclic prefix is a repetition of last data symbols in a transmitted block. By using CP, linear convolution of the channel impulse response and sent data block appears to be circular convolution at the receiver.

In OFDM systems inherently we are working in FD. To equalize a received block of symbols we use equalizers that are designed to work in FD. Adding cyclic prefix to the transmitted blocks thus obtaining circular structure at the receiver gives us opportunity to reduce the receiver complexity, because equalization can be done by simple complex multiplication per each sub-carriers. That is why OFDM systems have advantage of having simple receiver structure.

It is reported in [4] OFDM offer a better performance/complexity trade-off than conventional single carrier (SC) modulation with time domain equalization for large multpath spread. Also in [5] a comparison between three systems equalized Gaussian minimum shift keying (GMSK), equalized quadrature phase shift keying (QPSK) and

OFDM systems is carried out. It is reported that OFDM outperforms the other two systems. Another comparison between MC OFDM system and conventional SC system is reported in [6]. It is shown that for the assumed conditions coherent OFDM scheme provides about 2-3 dB performance gain compared to single-carrier modulation with lower complexity. It is also reported that in the receiver the most power consuming element regarding equalization is the equalizer for SC and the FFT for OFDM.

Although OFDM offers many advantages it has some limitations. Firstly, the efficiency of the transmission amplifier can be significantly limited due to the high peak-to-average power ratio of OFDM signal. Secondly, carrier synchronization is very important for OFDM systems. In order to obtain good performance each carrier must be synchronized very accurately.

1.1.2. SC Systems

When we suffer from the high peak-to-average power ratio problem of OFDM systems we can use some algorithms developed to alleviate this problem. Another solution is to use single-carrier systems instead of using MC systems. SC systems alleviates some problems that MC systems face, but they have disadvantage of having high complexity time domain (TD) equalizers.

One fundamental problem in high data rate wireless communication systems employing single carrier transmission is the equalization of the received signal. In wireless communication increasing data rate without taking any countermeasures means increasing the inter symbol interference (ISI). To combat whit ISI equalizers are being used [7]. In a conventional digital SC transmission systems these equalizers are designed in time domain. There are many ways to design a time domain equalizer. For example equalizers can be designed to work in an adaptive manner [8]. This kind of equalizers consist of one or more transversal filters with many taps. To perform equalization on each data symbol many multiplication must be carried out. Because of this huge number of multiplications we have high complexity receivers.

Similarly, sometimes communication is made by means of blocks. In situations like these, to perform equalization it is required to take an inverse of a matrix with large dimensions which increases the complexity. Although some complexity reducing algorithms were developed for broadband systems complexity is still too high [9].

A new technique to reduce the receiver complexity is to design some blocks of the receiver, such as channel estimator and equalizer, to work in frequency domain [10–12]. This new technique has some common elements with the OFDM systems. By doing some processes in frequency domain we use the low complexity advantage of the OFDM systems. In [13–15] Sari pointed out that, when combined with FFT processing and the use of cyclic prefix, a SC system with frequency domain equalizer (FDE) has essentially the same performance and low complexity as an OFDM system. Same results are obtained in [16] for FD single-carrier broadband wireless systems. Also in [17] it has been shown that FDE is more robust without interleaving and error-correction coding and less sensitive to nonlinear distortion and carrier synchronization difficulties which are main problems of the OFDM systems.

The FD equalization uses a similar reception technique that is used in OFDM systems. In these kind of systems communication is made block wise. To obtain periodic appearance of a transmitted block, a cyclic prefix is appended to each data block. This periodicity causes linear convolution of the channel and sent data block appear to be circular convolution. Thus, on the receiver side some operations such as channel estimation or equalization can be carried out with less multiplications.

In this thesis, we use this principle in UWB systems to decrease the receiver complexity. That is, we use frequency domain reception techniques not only for equalization purposes but also for channel estimation purpose.

For block transmission implementation of cyclic prefixed SC systems firstly we select the CP length so that it is equal or greater that the expected maximum channel delay spread. Next, we choose data block size long enough to make sure that channel variation is negligible over the block. This reduction of complexity comes with some

costs. The cyclic prefix length is an important parameter for this kind of systems. If it is not long enough, then IBI occurs between adjacent blocks. To avoid IBI, CP length must be equal or greater than the channel impulse response. However, we cannot choose the CP length as long as we want. Because, appending some prefix to the transmitted block causes reduction in bandwidth efficiency and power efficiency of our system. So the shorter the CP length, the better the bandwidth and power efficiency of a system. Especially, when our channel is highly time dispersive, usage of CP whose length is greater than channel impulse response causes huge amount of reductions of bandwidth and power efficiency of our system.

In literature there are some studies to solve this problem for SC systems. One solution proposal is to shorten the channel impulse response [18]. Another solution for performance degradation caused by usage of insufficient CP is to iteratively reconstruct missing CP on convolutionally encoded bit stream at receiver side [19]. Reconstruction gives good results but disadvantage is that we have a slight complexity increase because of reconstruction algorithm, but this increment of complexity does not take away our advantage of working in FD. In [20–22] there are other studies about the usage of insufficient CP with SC systems.

1.1.3. UWB Systems

Ultra-wideband (UWB) is a new communication technique that is a good candidate for short range multiple-access communications in dense multipath environments [23]. It is defined as any wireless transmission scheme that occupies a fractional bandwidth $W/f_c \geq 20\%$ where W is the transmission bandwidth and f_c is the band center frequency, or more than 500 MHz of absolute bandwidth. These systems use very narrow time duration baseband pulses of appropriate shape and duration to obtain such large bandwidths. Because of this large bandwidth, it is possible to obtain higher data rates without increasing transmit power or equivalently using sophisticated error control coding and higher order modulation schemes. This also means UWB systems are power efficient and it is possible to design low complexity receivers.

Impulse radio (IR) is a UWB technique that uses baseband pulses of very short duration, typically on the order of a nanosecond, thus spreading the energy of a radio signal very thinly from near dc to a few gigahertz [25]. A typical IR symbol is composed of many repeated pulses. This pulse repetition provides us with processing gain on receiver side. It becomes easier to detect and estimate transmitted symbols.

Currently in United States (US) for UWB wireless communication there are some regulations on power levels of pulses not to disturb currently operating systems such as global positioning systems (GPS) and wireless local area network WLAN [24].

Because of power limitation rules and multiple access issues, different spread spectrum (SS) techniques are applied to UWB systems. The two most common UWB transmission models are based on concept of time hopping spread spectrum (TH-SS) and direct sequence spread spectrum (DS-SS). Data information can be modulated by using pulse position modulation (PPM) or pulse amplitude modulation (PAM) [26–30].

The IR-UWB has a fine path resolution by transmitting information with ultra short pulses. Therefore, the RAKE receiver is known as a technique that can effectively combine paths with different delays and obtain path diversity [31]. In this kind of receivers there are as many correlators as the number of resolvable multipaths of the channel. It has been observed that in these kind of receivers energy capture is highly sensitive to the number of fingers (correlators) used in reception [32]. Since some UWB indoor channel have approximately 400 resolvable paths [33] it is unlikely that hundreds of correlators can be employed due to the practical reasons. So this kind of receivers are limited in performance.

As previously mentioned conventional antimultipath approach for single carrier transmission systems is to use TD equalizers. Since these equalizers uses as many filter taps as the number of resolvable paths their complexity is very high. That is why these equalizers are not suitable for UWB indoor communications. Especially, for non-line-of-sight (NLOS) UWB indoor channels where more than 400 multipaths exist [33].

Just as mentioned for SC systems one alternative to combat with multipath effect is to use FD equalizers in UWB systems. Recently there are some studies to use FD equalizer in UWB systems [34–37]. In all this studies CP length is assumed to be longer than channel impulse response. As we previously mentioned, using longer CP limits the bandwidth efficiency of a transmission system. Since UWB channels are highly time dispersive channels using sufficient CP length causes excessive badwidth efficiency lost.

In order to prevent this bandwidth efficiency lost, similar techniques that are being used in SC transmission can be used. For example, channel impulse response shortening can be applied or some reconstruction algorithms can be used. In [38] a reconstruction algorithm for UWB-IR and DS-UWB have been proposed. However, for reconstruction channel coefficients are assumed to known perfectly. In [39] the same authors investigated the effect of the imperfect channel estimation only on the performance of UWB-IR with the reconstruction algorithm proposed in [38].

1.1.4. Turbo Equalization

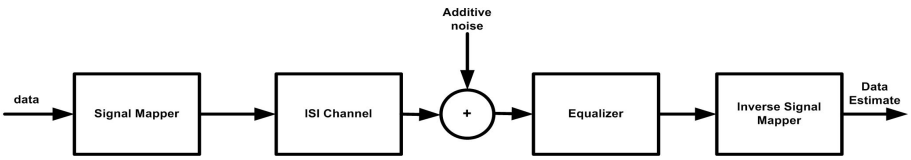

Figure 1.1. Representation of data transmission system

Turbo equalization principle is an efficient way of reception of transmitted symbols. In classical uncoded systems data are fed to the mapper and transmitted through ISI channel. The ISI is removed through equalization, and the data estimates are obtained from a mapper converting the hard decided equalized channel symbols to the input data alphabet as shown in Figure 1.1.

The optimal equalization method for minimizing the bit error rate and the sequence error rate are nonlinear and are based on maximum-likelihood (ML) estimation,

which turns into maximum a posteriori probability (MAP) in the presence of a priori information about the transmitted data. However, (MAP/ML) equalizers suffers from high complexity. For this reasons, equalization is done by using linear filters. The parameters of these filters can be selected according to many criteria such as zero forcing (ZF) or minimum-mean squared error (MMSE) criteria.

It is possible to increase the BER performance of a communication system by using coding. Block coding and convolutional codes are only two examples of present coding schemes. When coding is used on receiver side the decoder is fed either with hard or soft information. It is reported in [43] using soft information rather than hard information obtained from the equalizer increase the performance of the receiver. In these systems an interleaver is used after the encoder to shuffle symbols within a given block of data and thus decorrelates error event introduced by the equalizer between neighboring symbols. Correct ordering of symbols are obtained by using deinterleaver before the decoder.

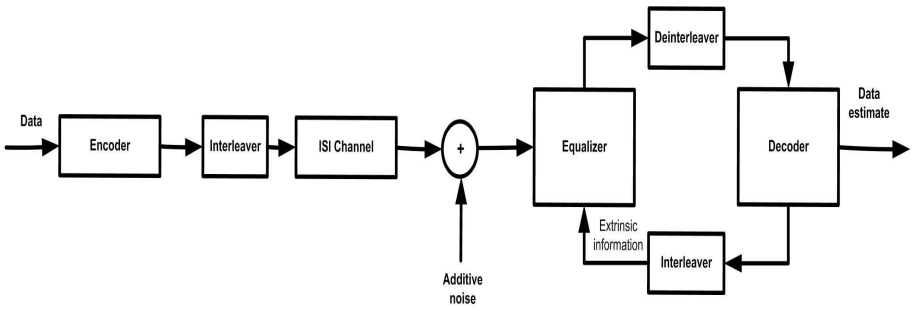

Figure 1.2. Data transmission using iterative (turbo) approach

Figure 1.2 depicts an example of an receiver based on iterative structure. In iterative algorithms the received data block is processed between at least two distinct processing blocks, such as an equalizer and a decoder. They are interacting with each other in both directions. A received block is processed several times until a predetermined convergence criteria is matched.

If we assume that the communication is done blockwise, the interleaver shuffles the code symbols of the encoder output. The deinterleaver reverses this step such that the

decoder reads the code symbols in the same ordering in which the encoder sent them. Also, the feedback information from the decoder is interleaved to provide the correct code symbol ordering for the equalizer. In this structure receiver's blocks are assumed to output soft information. One block of received data is repeatedly equalized and decoded using feedback from the decoder until previously assigned convergence criterion is met. One common problem of the iterative structures is the sensitivity to error propagation. This problem can be reduced by carefully choosing the outputs of the processing block i.e. communicating the extrinsic information between the processing blocks.

As we previously mentioned, using MAP equalization suffers from the high computational load especially for channel with long impulse response. This situation is exaggerated for the iterative structures, because a received block is processed several times. To overcome this problem Wang and Poor [44] used linear equalizer instead of MAP equalizer to remove ISI and MAP symbol estimator for decoding. Thus the MAP equalizer (exponential complexity) is replaced with an linear equalizer (LE, polynomial complexity). In [45] Tuchler proposed a MMSE equalizer that uses prior information in time domain for equalization of a received block. Although the MAP equalizer is replaced with MMSE equalizer, the computational load is still high for highly dispersive channel. It is because an inverse of a large matrix must be taken for the computation of the equalizer coefficients for every iteration. In order to further reduce the computations load in [45] Tuchler proposed a FD version of the MMSE equalizer proposed in [46].

1.2. Scope of the Thesis

In this thesis, we investigate the deteriorating effect of using short cyclic prefix on channel estimation and detection in binary pulse amplitude modulated (PAM) IR-UWB systems. We assume that the channel is unknown for the receiver and we used a pilot aided FD RLS channel estimation algorithm to estimate the channel. For the channel estimation we use FD RLS algorithm given in [47] and we propose an iterative scheme on this algorithm to compensate for the additional IBI caused by the usage of

the short CP. For the detection of the received symbols we use an iterative structure that is composed of FD MMSE equalizer proposed in [46] and pulse repetition decoder similar to decoder proposed in [48]. In order to compensate for the IBI error an additional IBI estimation block is used and it is combined with the whole system to operate in an iterative way for better reception of the transmitted symbols.

1.3. Outline of the Thesis

In Chapter 2, we present the signal model. In Chapter 3, the proposed receiver structure is presented. Also, the derivation of the proposed FD RLS channel estimation with IBI cancellation algorithm, FD equalizer and decoder is given in Chapter 3. Simulation results for channel estimation is also presented in Chapter 3. In addition, complexity analysis is given in Chapter 3. In Chapter 4, simulation results of the proposed receiver are given. Finally, conclusion is presented in Chapter 5.

2. SIGNAL MODEL

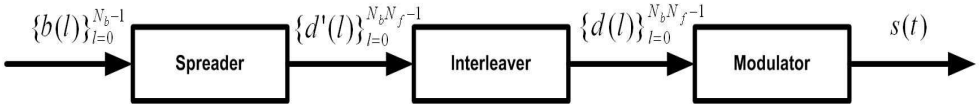

Figure 2.1. Representation of the transmitter

In our thesis we consider a single user uncoded chip-interleaved PAM IR-UWB system. The transmitter is depicted in Figure 2.1. The transmitter is a typical UWB transmitter. It consists of spreader, interleaver and a modulator. In a IR-UWB system signals are transmitted at baseband, so the transmitter complexity is fairly low compared to conventional communication systems. Following we give details of the signal model that we use in our system.

In a typical IR-UWB system, every symbol is transmitted over a duration of T_s in which N_f frames, each with a duration of T_f, are sent, i.e., $T_s = N_f T_f$. In each frame, a pule, $p(t)$, with a duration of $T_p = T_f$ is transmitted. With this model every information bit is repeated N_f times. This provides us with processing gain at the receiver side. In our study we investigate the deteriorating effect of using short CP. When CP length is shorter than the CIR length than there is a interference caused by the previously transmitted data blocks. To be able to define the amount of interference theoretically we use subscript 'n' to indicate the transmitted block index. Taking this notification into account at the transmitter the nth original input data sequence consisting of N_b bits is represented as $\mathbf{b}^n = \{b^n(l)\}_{l=0}^{N_b-1}$ where $b^n(l) \in \{+1, -1\}$. Each information bit is spread to $\mathbf{d}'^n = \{d'^n(l)\}_{l=0}^{N_bN_f-1}$ by repeating every bit N_f times. Thus $d'^n(l)$ can be expressed as

$$d'^n(l) = b^n\big(\lfloor \frac{l}{N_f} \rfloor\big) \tag{2.1}$$

Here $\lfloor . \rfloor$ denotes the integer floor operation. Then $\{d'^n(l)\}_{l=0}^{N_bN_f-1}$ is interleaved to $\mathbf{d}^n = \{d^n(l)\}_{l=0}^{N_bN_f-1}$ by using the interleaver denoted by $\prod$. After interleaving process

$d^n(l)$ is given by

$$d^n(l) = \prod \left(b^n\big(\lfloor \frac{l}{N_f} \rfloor\big) \right). \tag{2.2}$$

To insert CP last N_k element of the interleaved sequence $\mathbf{d}^n$, which are corresponding to chip positions, are inserted to the beginning of $\mathbf{d}^n$. Thus the transmitted signal is expressed as

$$s^n(t) = \sum_{l=-N_k}^{N_b N_f - 1} g^n(l) p(t - lT_f), \tag{2.3}$$

where $g^n(l) = d^n(< N_b N_f + l >_{N_b N_f})$, $< . >_{N_b N_f}$ is the modulo operation with respect to $N_b N_f$. The multipath channel is modelled as

$$h(t) = \sum_{m=0}^{\tilde{L}-1} \rho_m \delta(t - \tau_m)$$

where $\tilde{L}$ is the number of channel paths, ρ_m is the path gain and τ_m is the delay of the mth path. Sampling at frame rate T_f, the path delays τ_m can be approximated to the integer multiples of T_f. Accordingly, the fractionally spaced channel impulse function can be written as

$$h(t) = \sum_{l=0}^{L-1} h(l) \delta(t - lT_f)$$

where $L = \tau_{\tilde{L}-1}/T_f + 1$ with $\tau_{\tilde{L}-1}$ being the maximum path delay, and $h(l) = \rho_m$ for $l = \tau_m/T_f$ and zero for all other l values. Assuming that the receiver is fully synchronized and time delays are known, then the received signal for nth information bit sequence (block) can be expressed as

$$r^n(t) = s^n(t) * h(t) + w(t), \tag{2.4}$$

where * denotes linear convolution and $w(t)$ is AWGN with variance $N_0/2$. The continuous time received signal, $r(t)$, is passes through a chip-matched filter and sampled at the multiples of T_f yielding

$$r^n(m) = s^n(m) * h(m) + w(m), \qquad m = -N_k, \ldots, 0, \ldots N_b N_f - 1, \tag{2.5}$$

where $r(m)$, $s(m)$, $h(m)$ and $w(m)$ are the samples of chip-matched filter output, transmitted signal, channel impulse response and AWGN process respectively. There will be so called IBI depending on the CP length N_k is longer ($N_k > L$) or shorter ($N_k < L$) than the channel impulse response. Also another parameter that is affecting the IBI is the number of chips $N_b N_f$ (one pulse for each chip) contained in each transmitted block. In this thesis, we choose the length of each transmitted block to be constant over successive blocks and it is equal or greater than the channel impulse length, that is $N_b N_f \geq L$. By doing so we restrict the number of previously transmitted block that contribute to the IBI to be one. Derivation of the IBI term with this specifications is presented in appendix. The IBI error in nth block caused bay the *(n-1)*th block is as following

$$e^n(i) = \sum_{r=N_k+i}^{L-1} h(r)\Big\{ d^{n-1}\big(N_b N_f + N_k - 1 - i - r\big) - d^n\big(N_b N_f - r + i\big) \Big\}. \tag{2.6}$$

Also IBI derivation presented in appendix can be modified to contain two or more previously transmitted blocks.

If CP is longer than the channel impulse response then after removal of CP the received signal can be expressed as

$$r^n(i) = s^n(i) \star h(i) + w(i), \qquad i = 0, \ldots N_b N_f - 1, \tag{2.7}$$

where $\star$ represents circular convolution. However, if CP length is shorter than the channel impulse response additional IBI error term which given in (2.6) is added to the

received signal and it is expressed as

$$r^n(i) = s^n(i) \star h(i) + e^n(i) + w(i), \quad i = 0, \ldots N_b N_f - 1. \tag{2.8}$$

Equations (2.7) and (2.8) can be written in matrix form as

$$\begin{aligned} \mathbf{r}^n &= \mathbf{H}_C \mathbf{d}^n + \mathbf{w}, \\ &= \mathbf{H}_C \mathbf{d}^n + \mathbf{e}^n + \mathbf{w}, \end{aligned} \tag{2.9}$$

where $\mathbf{r}^n$ is a $(N_b N_f \times 1)$ column vector containing samples of the received signal, $\mathbf{H}_C$ is a $(N_b N_f \times N_b N_f)$ circular matrix whose elements are the channel impulse response, subscript C stands for circular matrix, $\mathbf{d}^n$ is a $(N_b N_f \times 1)$ composed of the chip values of the nth transmitted block, $\mathbf{w}$ is a $(N_b N_f \times 1)$ column vector that contains AWGN samples and $\mathbf{e}^n$ is a $(N_b N_f \times 1)$ column vector that contains IBI error terms, and are expressed as follow

$$\begin{aligned} \mathbf{r}^n &= [r^n(0) \quad r^n(1) \quad r^n(2) \quad ... \quad r^n(N_b N_f - 1)]^T, \\ \mathbf{d}^n &= [d^n(0) \quad d^n(1) \quad d^n(2) \quad ... \quad d^n(N_b N_f - 1)]^T, \\ \mathbf{e}^n &= [e^n(0) \quad e^n(1) \quad e^n(2) \quad ... \quad e^n(N_b N_f - 1)]^T, \\ \mathbf{w} &= [w(0) \quad w(1) \quad w(2) \quad ... \quad w(N_b N_f - 1)]^T, \end{aligned} \tag{2.10}$$

$$\mathbf{H_C} = \begin{bmatrix} h(0) & 0 & \dots & 0 & h(L-1) & h(L-2) & \dots & h(2) & h(1) \\ h(1) & h(0) & 0 & \dots & 0 & h(L-1) & \dots & h(3) & h(2) \\ h(2) & h(1) & h(0) & 0 & \dots & 0 & \ddots & \dots & h(3) \\ \vdots & \ddots & \ddots & \ddots & \ddots & \ddots & \ddots & \ddots & \vdots \\ \vdots & \ddots & \ddots & \ddots & \ddots & \ddots & \ddots & \ddots & h(L-1) \\ h(L-1) & h(L-2) & \dots & \dots & \dots & h(0) & 0 & \dots & 0 \\ 0 & \ddots & \ddots & \ddots & \ddots & \ddots & \ddots & \ddots & \vdots \\ \vdots & \ddots & \ddots & \ddots & \ddots & \ddots & \ddots & h(0) & 0 \\ 0 & \dots & 0 & 0 & h(L-1) & \dots & h(2) & h(1) & h(0) \end{bmatrix}.$$

An alternative forms of (2.9) which will be used to derive RLS channel estimation algorithm, can be written. As we see, the the first terms on the right hand side of the equality is $\mathbf{H}_C\mathbf{d}^n$. This expression can be changed to be $\mathbf{D}_C^n\mathbf{h}$, where $\mathbf{h}$ is a $(N_bN_f \times 1)$ column vector whose elements are

$$\mathbf{h} = [h(0) \quad h(1) \quad h(2) \quad ... \quad h(L-1) \quad 0 \quad ... \quad 0)]^T \tag{2.11}$$

and $\mathbf{D}_C^n$ is a $(N_bN_f \times N_bN_f)$ circular matrix expressed as

$$\mathbf{D}_C^n = \begin{bmatrix} d^n(0) & d^n(N_bN_f-1) & \dots & d^n(3) & d^n(2) & d^n(1) \\ d^n(1) & d^n(0) & d^n(N_bN_f-1) & \dots & d^n(3) & d^n(2) \\ d^n(2) & d^n(1) & d^n(0) & \dots & d^n(4) & d^n(3) \\ \vdots & \ddots & \ddots & \ddots & \ddots & \vdots \\ d^n(N_bN_f-2) & \dots & \dots & d^n(1) & d^n(0) & d^n(N_bN_f-1) \\ d^n(N_bN_f-1) & \dots & \dots & d^n(2) & d^n(1) & d^n(0) \end{bmatrix}.$$

Using this alternative form, (2.9) can be written as

$$\begin{aligned} \mathbf{r}^n &= \mathbf{D}_C^n\mathbf{h} + \mathbf{w}, \\ &= \mathbf{D}_C^n\mathbf{h} + \mathbf{e}^n + \mathbf{w}. \end{aligned} \tag{2.12}$$

Since channel estimation and equalization is done in FD, (2.9) and (2.12) need to be transformed to FD. The advantage of these equations lies under the circular structures of matrices $\mathbf{H}_C$ and $\mathbf{D}_C^n$. Since they are circular matrices they can be expressed as $\mathbf{H}_C = \mathbf{F}^H \Psi \mathbf{F}$, where $\mathbf{F}$ is the discrete Fourier transform (DFT) matrix and $F_{l,k} = \frac{1}{\sqrt{N_b N_f}} exp\Big(- j\frac{2\pi}{N_b N_f} lk \Big), 0 \leq l,k \leq N_b N_f - 1$ and Ψ is $(N_b N_f x N_b N_f)$ diagonal matrix, with its *(k,k)*th entry as

$$\psi_k = \sum_{l=0}^{N_b N_f - 1} h(l) exp\Big(- j\frac{2\pi}{N_b N_f} lk \Big)$$

similarly $\mathbf{D}_C^n$ can be written as $\mathbf{D}_C^n = \mathbf{F}^H \mathbf{M}^n \mathbf{F}$ here $\mathbf{M}^n$ is $(N_b N_f x N_b N_f)$ diagonal matrix, with its *(k,k)*th entry as

$$M_k^n = \sum_{l=0}^{N_b N_f - 1} d^n(l) exp\Big(- j\frac{2\pi}{N_b N_f} lk \Big).$$

Using these facts the last line of (2.12) can be written in FD as

$$\begin{aligned} \mathbf{F}\mathbf{r}^n &= \mathbf{F}(\mathbf{H}_C \mathbf{d}^n) + \mathbf{F}\mathbf{e}^n + \mathbf{F}\mathbf{w}, \\ &= \mathbf{F}(\mathbf{F}^H \Psi \mathbf{F}\mathbf{d}^n) + \mathbf{F}\mathbf{e}^n + \mathbf{F}\mathbf{w}, \\ \mathbf{R}^n &= \Psi \mathbf{D}^n + \mathbf{E}^n + \mathbf{W}. \end{aligned} \tag{2.13}$$

where $\mathbf{R}^n = \mathbf{F}\mathbf{r}^n$, $\mathbf{D}^n = \mathbf{F}\mathbf{d}^n$, $\mathbf{E}^n = \mathbf{F}\mathbf{e}^n$ and $\mathbf{W} = \mathbf{F}\mathbf{w}$. Similarly (2.9) and the first line of (2.12) can be written in FD respectively as

$$\begin{aligned} \mathbf{R}^n &= \Psi \mathbf{D}^n + \mathbf{W}, \\ &= \mathbf{M}^n \mathbf{H} + \mathbf{W}, \\ &= \mathbf{M}^n \mathbf{H} + \mathbf{E}^n + \mathbf{W}. \end{aligned} \tag{2.14}$$

This representations of the received signal are used during the derivations of FD RLS channel estimation, FD equalization and symbol detection algorithms. In the following chapter we explain the proposed receiver structure.

3. CHANNEL ESTIMATION, EQUALIZATION AND DECODING

In this chapter we explain the proposed receiver structure when short CP is used causing IBI. The proposed receiver structure is shown in Figure 3.1. It is composed of FD RLS channel estimator, FD SISO MMSE equalizer, repetition decoder and IBI error estimator.

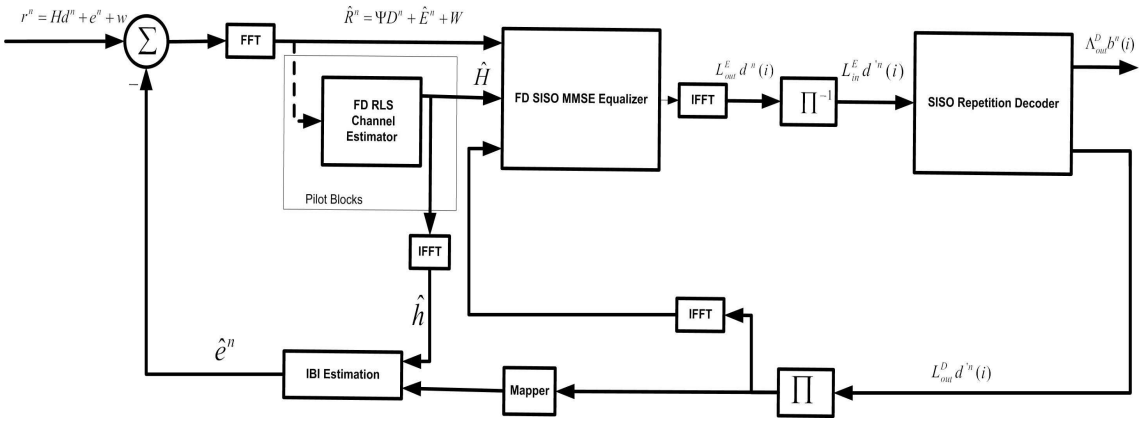

Figure 3.1. Block diagram of the proposed receiver

The channel estimation is done in frequency domain by using pilot blocks. For channel estimation we propose an iterative scheme that is based on cancelling IBI error iteratively. For the equalization of the received data blocks we propose to use FD SISO MMSE equalizer. Decoding is done by using repetition decoder that accepts soft outputs of the equalizer as input and produces soft outputs. The IBI cancellation is done by estimating the IBI error and subtracting it from the received block in next iteration. In following sections we explain the details of each receiver components in details.

3.1. Frequency Domain Recursive Least Squares Channel Estimation With Inter Block Interference Cancellation

The RLS channel estimation is one of the channel estimation method widely used in literature. In our study, we prefer the RLS algorithm because it has better convergence properties than most of its counter parts. However, it can be changed with another FD channel estimation algorithm such as FD least mean squares (LMS) given in [47] with lower complexity but with slower convergence rate. We use the FD version of RLS algorithm proposed in [47]. In order to compensate for the IBI error we made some modifications on this algorithm. If we consider the last line of (2.14) which represents the received signal for short CP usage the RLS aims at minimizing the exponentially weighted sum

$$J_{RLS}(\tilde{\mathbf{H}}) = \sum_{i=0}^{n} \lambda^{n-i} \|\mathbf{R}^i - \mathbf{M}^i \tilde{\mathbf{H}}\|^2, \tag{3.1}$$

where $0 < \lambda < 1$ is the forgetting factor. The minimum is achieved for $\tilde{\mathbf{H}} = \hat{\mathbf{H}}^n$, with $\hat{\mathbf{H}}^n$ satisfying the the recursive equation

$$\hat{\mathbf{H}}^{n+1} = \hat{\mathbf{H}}^n + \mathbf{K}^n \mathbf{z}^n, \tag{3.2}$$

where $\mathbf{z}^n = (\mathbf{M}^n)^H [\mathbf{R}^n - \mathbf{M}^n \hat{\mathbf{H}}^n]$ and $\mathbf{K}^n = diag[K^n(0) \quad K^n(1) \quad ... \quad K^n(N_b N_f - 1)]$. The term $K^n(i)$ is expressed by

$$K^n(i) = \frac{S^n(i)}{\lambda + |M_i^n|^2 S^n(i)}, \qquad i = 0, \ldots, N_b N_f - 1, \tag{3.3}$$

with $S^n(i)$ satisfying the recursion

$$S^{n+1}(i) = \frac{1}{\lambda} S^n(i) \left[1 - K^n(i) |M_i^n|^2 \right], \; i = 0, \ldots, N_b N_f - 1. \tag{3.4}$$

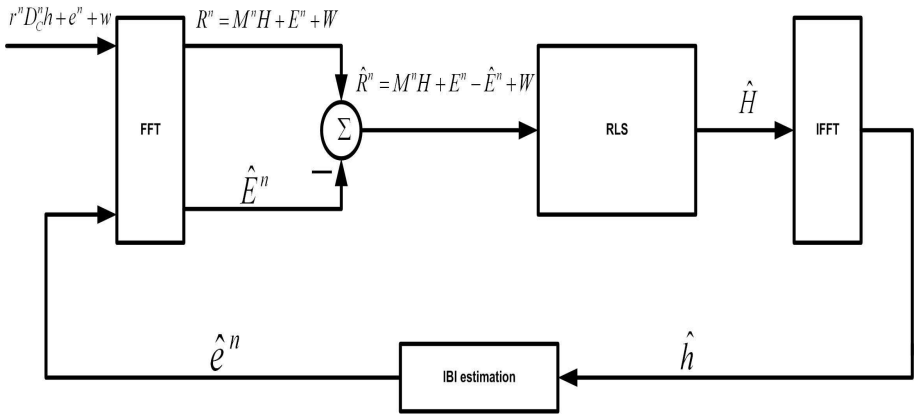

Figure 3.2. FD Channel estimation with IBI cancellation

In our study we assume that, the channel estimation is done by using training blocks. Modification is done by estimating the IBI error as $\hat{\mathbf{E}}^n$ and subtracting it from the FD received signal as shown in Figure 3.2. In this way the estimate of the received signal is obtained and it is used as an input for the next iteration of the RLS algorithm. Since the IBI error e^n is defined in time domain as shown in (2.6), the IBI estimation is done in time domain and converted to frequency domain. Although this estimation process slightly increases the channel estimation complexity, it provides us with better channel estimation by iteratively cancelling IBI error. It is observed in (2.6) that the required parameters to be able to estimate e^n are channel impulse responses, currently and previously transmitted symbol blocks. The channel estimation is assumed to be done via pilot blocks. When this is the case, currently and previously transmitted symbol blocks are known. Remaining unknown parameter is the channel impulse responses (CIR). In our proposed algorithm we use estimated channel coefficients from the previous iteration to estimate the IBI error. Then we subtract this estimated IBI error from the received signal in the next iteration.

In (2.6) it is also observed that not all the IBI error terms are affected by the CIR equally. The number of CIR coefficients that affects the IBI error term decreases when the IBI error term index increases. To compensate for this effect a new parameter is defined to be energy coefficient and it is the ratio of the energy of the estimated channel coefficients from previous iteration those affecting the ith IBI error term to the energy

of the all estimated channel coefficients from the previous iteration.

$$a^n(i) = \frac{\sum_{r=N_k+i}^{L-1} \hat{h}^2(r)}{\sum_{j=0}^{L-1} \hat{h}^2(j)}.$$

A similar parameter is present in [38]. By using the estimated CIR coefficients and the energy coefficient the IBI error estimation is done with the following equation

$$\hat{e}^n(i) = a^n(i) \sum_{r=N_k+i}^{L-1} \hat{h}^n(r)\{b^{n-1}(N_bN_f + N_k - 1 + i - r) - b^n(N_bN_f - r + i)\}. \quad (3.5)$$

During the simulations it is observed that if energy coefficient is not used for IBI error estimation some convergence problems are faced because of the feedback structure that is used for channel estimation. The combined IBI error cancelation with RLS algorithm is as following

Step 1: Initialize $\hat{\mathbf{h}}$ and $S^n(i) \qquad i = 0, \ldots, N_bN_f - 1$

Step 2: Calculate IBI $\hat{\mathbf{e}}^n$ using (3.5)

Step 3: Calculate the FFT of $\hat{\mathbf{e}}^n \rightarrow \hat{\mathbf{E}}^n$

Step 4: Subtract estimated IBI error $\hat{\mathbf{E}}^n$ from received vector $\mathbf{R}^n$ obtain estimate of received vector $\hat{\mathbf{R}}^n$

$$\hat{\mathbf{R}}^n = \mathbf{M}^n\mathbf{H} + \mathbf{E}^n - \hat{\mathbf{E}}^n + \mathbf{W} \quad (3.6)$$

Step 5: Calculate $\mathbf{z}^n = (\mathbf{M}^n)^H[\hat{\mathbf{R}}^n - \mathbf{M}^n\hat{\mathbf{H}}^n]$
for first iteration when $n = 1$ use frequency domain values of initially assigned $\hat{\mathbf{h}}^n$ channel coefficient in first step.

Step 6: Calculate $K^n(i)$ for $i = 0, \ldots, N_bN_f - 1$, using (3.3)

Step 7: Calculate $\hat{\mathbf{H}}^{n+1}$ using (3.2)

Step 8: Calculate $S^{n+1}(i)$ for $i = 0, \ldots, N_bN_f - 1$, using (3.4)

Step 9: Calculate the IFFT of $\hat{\mathbf{H}}^n \rightarrow \hat{\mathbf{h}}^n$ and go to *step 2* in order to calculate IBI error with these new channel coefficients.

3.1.1. Simulation Results for Channel Estimation

In this section the simulation results for proposed FD RLS channel estimation are presented. In all simulations, channel model four (CM4) [33] is used as the multipath channel which has 360 taps leading to a severe ISI. In order to interleave the data blocks random interleaver is used. Pulse and chip durations are set equal to 1ns, i.e. $T_p = T_f = T_c = 1ns$. Each transmitted block is composed of 160 information bits. Each information bit is spread over 4 chips, i.e. to transmit an information bit 4 pulse with 1ns. duration is used. Whit this set up each block consists of 640 chips (pulse). On receiver side matched filter outputs are sampled with sampling rate of 1ns. thus each received block has 640 samples. In simulations forgetting factor, λ, is set to be 0.9999 As a performance criterion for channel estimation normalized mean squared error is used, and it is defined as

$$NMSE(\hat{\mathbf{H}}) \triangleq \frac{E\{\|\mathbf{H} - \hat{\mathbf{H}}\|^2\}}{E\{\|\mathbf{H}\|^2\}}.$$

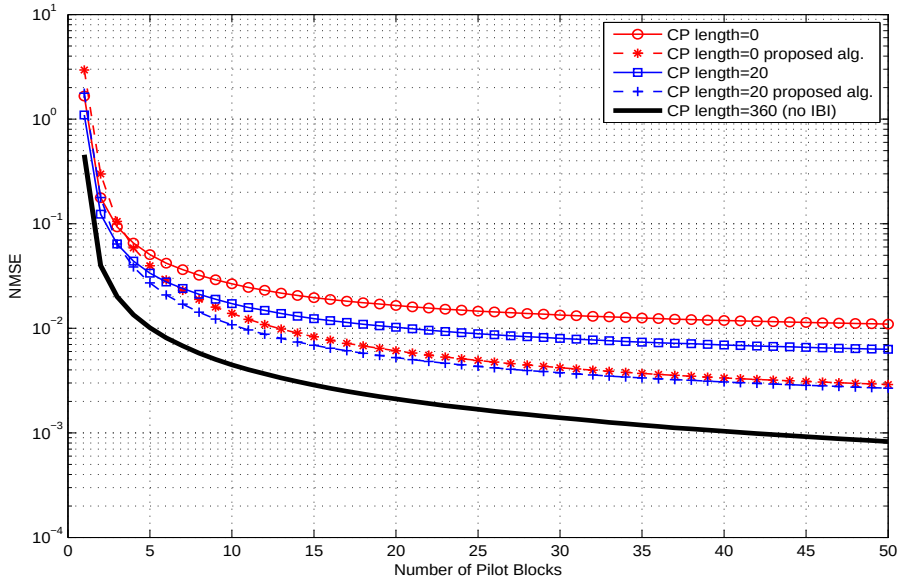

Figure 3.3. FD Channel estimation with IBI cancellation, number of pulse repetition=4 block size=160 symbols (640 chips) channel length=360 taps SNR=20 dB

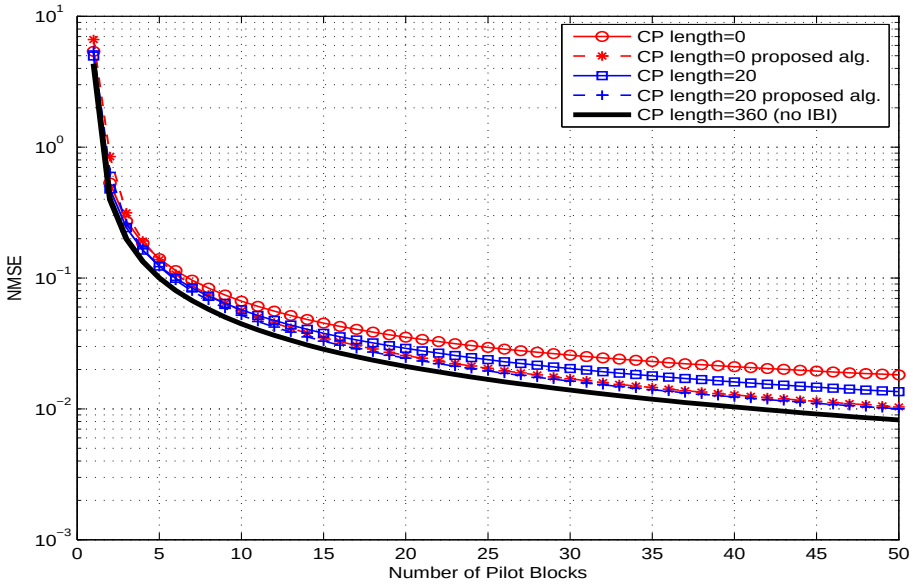

Figure 3.4. FD Channel estimation with IBI cancellation, number of pulse repetition=4 block size=160 symbols (640 chips) channel length=360 taps SNR=10 dB

Figure 3.3 shows the channel estimation results for full CP $N_k = 360$, no CP $N_k = 0$ and short CP $N_k = 20$ cases together with the proposed algorithm at 20 dB SNR. Notice that, using the specifications given above there is a one to one matching between each channel tap and each chip positions. The CP length is defined in terms of chip positions. If the CP length is equal or greater than the channel impulse then there is no IBI. It is observed in Figure 3.3 that, when CP length is 360 NMSE is on order of 10^{-3} after 50 pilot blocks. The channel estimation performance decreases when CP length decreases. It is also observed that there is a substantial increase in channel estimation performance with the proposed IBI cancelation algorithm. Similarly Figure 3.4 shows results for channel estimation at 10 dB SNR. The estimation characteristic for channel estimation at 10 dB is the same with the estimation characteristic at 20 dB but the performance decreases as expected. Although the estimation performance improvement is more for 20 dB SNR, estimation results are more close to that of sufficient CP case at 10 dB SNR. It is because of that, at low SNR's the error caused by AWGN is more dominant than that of IBI error. This causes the margin between

no CP case and sufficient CP case to decrease. Thus even if we have a small amount of improvement with proposed algorithm, obtained estimation results are closer to that of sufficient CP case.

3.2. Frequency Domain Soft Input Soft Output Minimum Mean Squares Error Equalizer

For the recovery of the transmitted data in the presence of ISI and noise we use FD SISO minimum mean squares linear equalizer algorithm proposed in [46]. The time domain version of the the SISO MMSE-LE is derived in [45]. Given the received vector for nth data block $\mathbf{r}^n$ and extrinsic LLR about the chip positions $\{L_{in}^E(d^n(i))\}_{i=0}^{N_bN_f-1}$ (which are computed by the decoder) the SISO MMSE-LE computes estimates of chip values $\hat{d}^n(i)$ of the transmitted data bits by minimizing cost function $E(|d^n(i)-\hat{d}^n(i)|^2)$. The MMSE-LE also produces LLR of chip values $\{L_{out}^E(d^n(i))\}_{i=0}^{N_bN_f-1}$. The estimates $\hat{d}^n(i)$ are computed as [45]

$$\begin{aligned} \mathbf{c} &= Cov(\mathbf{r}^n, \mathbf{r}^n)^{-1} Cov(\mathbf{r}^n, d^n(i)), \\ \hat{d}^n(i) &= E\{d^n(i)\} + \mathbf{c}^T(\mathbf{r}^n - E\{\mathbf{r}^n\}), \end{aligned} \tag{3.7}$$

where $E\{d^n(i)\}$ is given as

$$\bar{d}^n(i) = E\{d^n(i)\}, \tag{3.8}$$

which are obtained from the decoder and the derivation is given in following sections. In order to derive the FD version of the MMSE-LE algorithm [45] the approximate implementation of the time domain algorithm is used where the equalizer coefficients $\mathbf{c}$ are computed under the assumption that $d^n(i)$ are equally likely +1 or -1 yielding $E\{d^n(i)\} = 0$ and they are kept constant over the iterations. Therefore

$$\begin{aligned} Cov(\mathbf{r}^n, \mathbf{r}^n) &= \sigma_w^2 \mathbf{I}_{N_bN_f} + \mathbf{H}_C \mathbf{H}_C^H, \\ Cov(\mathbf{r}^n, d^n(i)) &= \mathbf{H}_C \mathbf{u}, \end{aligned} \tag{3.9}$$

where $\mathbf{u} = [1\mathbf{0}_{1\times N_bN_f-1}]$. Thus time invariant coefficients $\mathbf{c}$ is

$$\mathbf{c} = \left(\sigma_w^2\mathbf{I}_{N_bN_f} + \mathbf{H}_C\mathbf{H}_C^H\right)^{-1}\mathbf{H}_C\mathbf{u}. \tag{3.10}$$

If we collect the expected values of each chip positions $E\{d^n(i)\}$ in a vector $\bar{d}^n$ as

$$\begin{aligned} \bar{\mathbf{d}}^n &= \left[E\{d^n(0)\} \quad E\{d^n(1)\} \quad E\{d^n(2)\} \quad ... \quad E\{d^n(N_bN_f-1)\}\right]^T, \\ &= \left[\bar{d}^n(0) \qquad \bar{d}^n(1) \qquad \bar{d}^n(2) \qquad ... \qquad \bar{d}^n(N_bN_f-1)\right]^T, \end{aligned} \tag{3.11}$$

and using (3.7),(3.10) and (3.11) estimate of the ith chip position can be expressed as

$$\hat{d}^n(i) = \mathbf{c}^T\left(\mathbf{r}^n - \mathbf{H}_C\bar{\mathbf{d}}^n + \bar{d}^n(i)\mathbf{H}_C\mathbf{u}\right). \tag{3.12}$$

If the estimates of the chip positions are put in a matrix form

$$\hat{\mathbf{d}}^n = \left[\hat{d}^n(0) \quad \dots \quad \hat{d}^n(N_bN_f-1)\right]^T \tag{3.13}$$

and we define $\mathbf{p} = \mathbf{H}_C^H\mathbf{c}$ then estimates of the chip positions can be written as [46]

$$\hat{\mathbf{d}}^n = (\mathbf{Circ}_{N_bN_f}[\mathbf{c}])^H\mathbf{r}^n - (\mathbf{Circ}_{N_bN_f}[\mathbf{p}])^H\bar{\mathbf{d}}^n + \mathbf{p}^H\mathbf{u}\bar{\mathbf{d}}^n, \tag{3.14}$$

where $\mathbf{Circ}_{N_bN_f}$ represent a $N_bN_f \times N_bN_f$ circular matrix. The advantage of the (3.14) is the circular structures of terms $\mathbf{Circ}_{N_bN_f}[\mathbf{c}]$ and $\mathbf{Circ}_{N_bN_f}[\mathbf{p}]$. If DFT is applied to (3.14) by multiplying with a matrix defined as

$$\mathbf{T} = t_{n,k}, \quad n,k = 0,1,\dots,N_bN_f-1, \quad t_{n,k} = exp(-j\frac{2\pi nk}{N_bN_f}), \tag{3.15}$$

where $j = \sqrt{-1}$. Using the fact that $(N_bN_f)\mathbf{T}^{-1}\mathbf{T} = \mathbf{T}^H\mathbf{T} = (N_bN_f)\mathbf{I}_{N_bN_f}$

$$\begin{aligned}
\mathbf{C} &= \mathbf{Tc} = [C_0 \dots C_{N_bN_f-1}]^T, \\
\Lambda &= \mathbf{T}[h_0 h_1 \dots h_{L-1}\mathbf{0}_{1\times N_bN_f-L}]^T = [\Lambda_0 \dots \Lambda_{N_bN_f-1}]^T, \\
\mathbf{P} &= \mathbf{Tp} = \mathbf{TT}^{-1}\mathbf{Diag}[\Lambda]^H\mathbf{Tc} = \mathbf{Diag}[\Lambda]^H\mathbf{C} = \left[(C_0.\Lambda_0) \dots (C_{N_bN_f-1}.\Lambda_{N_bN_f-1})\right]^T, \\
\hat{\mathbf{D}}^n &= \mathbf{T}\hat{\mathbf{d}}^n = \mathbf{T}\big(\mathbf{Circ}_{N_bN_f}(\mathbf{c})\big)^H\mathbf{T}^{-1}\mathbf{Tr} - \mathbf{T}\big(\mathbf{Circ}_{N_bN_f}(\mathbf{p})\big)^H\mathbf{T}^{-1}\mathbf{T}\bar{\mathbf{d}}^n + \mathbf{Tp}^H\mathbf{u}\bar{\mathbf{d}}^n, \\
&= \mathbf{Diag}[\mathbf{C}]^H\mathbf{Tr}^n - \mathbf{Diag}[\mathbf{P}]^H\mathbf{T}\bar{\mathbf{d}}^n + \frac{1}{N_bN_f}.\mathbf{TP}^H\mathbf{Tu}\bar{\mathbf{d}}^n, \\
&= \mathbf{Diag}[\mathbf{C}]^H\mathbf{Tr}^n - \mathbf{Diag}[\mathbf{P}]^H\mathbf{T}\bar{\mathbf{d}}^n + \frac{1}{N_bN_f}.\sum_{k=0}^{N_bN_f}(C_k.\Lambda_k)\mathbf{T}\bar{\mathbf{d}}^n.
\end{aligned} \tag{3.16}$$

the vector $\mathbf{C}$ can be written in terms of Λ as

$$\begin{aligned}
\mathbf{C} &= \mathbf{Tc} = \mathbf{T}\big(\sigma_w^2\mathbf{I}_{N_bN_f} + \mathbf{H}_C\mathbf{H}_C^H\big)^{-1}\mathbf{H}_C\mathbf{u}, \\
&= \mathbf{T}\big(\sigma_w^2\mathbf{I}_{N_bN_f} + \mathbf{T}^{-1}\mathbf{Diag}[\Lambda]\mathbf{Diag}[\Lambda]^H\mathbf{T}\big)^{-1}\mathbf{T}^{-1}\mathbf{Diag}[\Lambda]\mathbf{Tu}, \\
&= \big(\sigma_w^2\mathbf{I}_{N_bN_f} + \mathbf{Diag}[\Lambda]\mathbf{Diag}[\Lambda]^H\big)^{-1}\mathbf{Diag}[\Lambda]\mathbf{1}_{N_bN_f}.
\end{aligned} \tag{3.17}$$

Thus the SISO MMSE equalizer coefficients can be easily calculated as

$$C_k = \frac{\Lambda_k}{(\sigma_w^2) + \Lambda_k\Lambda_k^*}, \qquad k = 0, \dots, N_bN_f - 1. \tag{3.18}$$

After computing the FD estimates of $\hat{\mathbf{D}}^n$ we go to the time domain to compute log-likelihood ratio (LLR) of chip values $d^n(i)$. In order to compute the LLRs of the chip values the mean and variance of the estimation error is obtained as in [45]

$$\mu = \mathbf{c}^H\mathbf{H}_C\mathbf{u} = \mathbf{p}^H\mathbf{u} = \frac{1}{N_bN_f}\mathbf{P}^H\mathbf{Tu} = \frac{1}{N_bN_f}.\sum_{k=0}^{N_bN_f-1}(C_k^*.\Lambda_k), \tag{3.19}$$

$$\hat{\sigma}^2 = \frac{1}{N_bN_f}\sum_{k=0}^{N_bN_f-1}|sign(\hat{d}^n(i)).\mu - \hat{d}^n(i)|^2, \tag{3.20}$$

and equalizer outputs are computed as

$$L_{out}^{E}\big(d^{n}(i)\big) = \frac{2\hat{d}^{n}(i)\mu}{\hat{\sigma}^{2}}. \tag{3.21}$$

For the first equalization step, no extrinsic information is available from the decoder the equalizer assumes in that case $\big\{L_{in}^{E}\big(d^{n}(i)\big) = 0\big\}_{i=0}^{N_bN_f-1}$ and uses

$$L_{out}^{E}\big(d^{n}(i)\big) = \frac{2\hat{d}^{n}(i)}{1-\mathbf{u}^{H}\mathbf{H}_{C}^{H}\mathbf{c}} = \frac{2\hat{d}^{n}(i)}{1-\mu^{*}}. \tag{3.22}$$

The algorithm is composed of two stages for the first stage there is no extrinsic information obtained from the decoder and they are assumed to be zero. Table 3.1 shows the algorithm in the absence of extrinsic information.

Table 3.1. FD MMSE equalization algorithm in the absence of extrinsic information

Input: received symbols $[r^{n}(0)\dots r^{n}(N_bN_f-1)]^{T}$, channel $h(k)$ and σ_w^2,

Initialization:

$$\begin{aligned}
[R^{n}(0)\dots R^{n}(N_bN_f-1)]^{T} &\leftarrow DFT[r^{n}(0)\dots r^{n}(N_bN_f-1)]^{T},\\
[\Lambda_0\dots\Lambda_{N_bN_f-1}]^{T} &\leftarrow DFT[h(0)\dots h(L-1)0\dots 0],\\
\mu &\leftarrow \frac{1}{N_bN_f}\sum_{k=0}^{N_bN_f-1}\frac{\Lambda_k\Lambda_k^{*}}{\sigma_w^2+\Lambda_k\Lambda_k^{*}},
\end{aligned}$$

Equalization:

$$\begin{aligned}
\hat{D}^{n}(k) &\leftarrow \frac{\Lambda_k\Lambda_k^{*}}{\sigma_w^2+\Lambda_k\Lambda_k^{*}}R^{n}(k) \quad k=0,1,\dots,N_bN_f-1,\\
[\hat{d}^{n}(0)\dots\hat{d}^{n}(N_bN_f-1)]^{T} &\leftarrow DFT^{-1}[\hat{D}^{n}(0)\dots\hat{D}^{n}(N_bN_f-1)]^{T},\\
L_{out}^{E}\big(d^{n}(k)\big) &\leftarrow \frac{2\hat{d}^{n}(k)}{1-\mu^{*}}.
\end{aligned}$$

During the second stage we have extrinsic LLR of each chip position obtained from the decoder. Table 3.2 shows the algorithm when extrinsic information is available.

Table 3.2. FD MMSE equalization algorithm using extrinsic information

Input: received symbols $[r^n(0)\dots r^n(N_bN_f-1)]^T$, channel $h(k)$, σ_w^2 and extrinsic LLR from the decoder $L_{in}^E\big(d^n(k)\big) = L_{out}^D\big(d^n(k)\big)$,

Initialization:

$$\begin{aligned}
[R^n(0)\dots R^n(N_bN_f-1)]^T &\leftarrow DFT[r^n(0)\dots r^n(N_bN_f-1)],\\
[\Lambda_0\dots\Lambda_{N_bN_f-1}]^T &\leftarrow DFT[h(0)\dots h(L-1)0\dots 0],\\
\mu &\leftarrow \frac{1}{N_bN_f}\sum_{k=0}^{N_bN_f-1}\frac{\Lambda_k\Lambda_k^*}{\sigma_w^2+\Lambda_k\Lambda_k^*},
\end{aligned}$$

Equalization:

$$\begin{aligned}
\bar{d}^n(k) &\leftarrow tanh\left(\frac{1}{2}L_{in}^E\big(d^n(k)\big)\right),\\
[\bar{D}^n(0)\dots\bar{D}^n(N_bN_f-1)]^T &\leftarrow DFT[\bar{d}^n(0)\dots\bar{d}^n(N_bN_f-1)]^T,\\
\hat{D}^n(k) &\leftarrow \frac{\Lambda_k\Lambda_k^*}{\sigma_w^2+\Lambda_k\Lambda_k^*}R^n(k)+(\mu-\frac{\Lambda_k\Lambda_k^*}{\sigma_w^2+\Lambda_k\Lambda_k^*})\bar{D}^n(k),\\
[\hat{d}^n(0)\dots\hat{d}^n(N_bN_f-1)]^T &\leftarrow DFT^{-1}[\hat{D}^n(0)\dots\hat{D}^n(N_bN_f-1)]^T,\\
\hat{\sigma}^2 &\leftarrow \frac{1}{N_bN_f}\sum_{k=0}^{N_bN_f-1}\big|sign\big(\hat{d}^n(k)\big).\mu-\hat{d}^n(k)\big|^2,\\
L_{out}^E\big(d^n(k)\big) &\leftarrow \frac{2\hat{d}^n(k)\mu}{\hat{\sigma}^2}.
\end{aligned}$$

After obtaining LLR of each chip positions they are deintereaved and fed to the SISO repetition decoder explained in next section.

3.3. Soft Input Soft Output Repetition Decoder

Different than conventional systems in which convolutional coding is used for error control coding (ECC) in our system we don't have convolutional codes. Instead we use pulse repetition structure as a kind of ECC. So the decoder is repetition decoder similar to [48]. The main task of the decoder is to generate extrinsic information about he chip values which are provided to the IBI estimator and SISO MMSE equalizer and to produce estimates of the transmitted information bit in last iteration. As previously stated the LLR outputs of the equalizer is

$$L_{out}^{E}\big(d^{n}(i)\big) = \frac{2\hat{d}^{n}(i)\mu}{\hat{\sigma}^{2}} \quad i = 0, 1, \ldots, N_b N_f - 1. \tag{3.23}$$

After deinterleaving $L_{out}^{E}\big(d'^{n}(i)\big) = \Pi^{-1}\Big(L_{out}^{E}\big(d^{n}(i)\big)\Big)$. Next they are fed to the decoder as the a priori information. If we concentrate on chips related to ith bit $b^{n}(i)$. Recall that $b^{n}(i)$ is spread into the chips sequence $\{d'^{n}(j)\}_{j\in\chi_i}$ where

$$\chi_i = \{N_f i, N_f i + 1, \ldots, N_f i + N_f - 1\}$$

due to the interleaver $L_{out}^{E}\big(d'^{n}(j)\big)$ are assumed uncorrelated. Using the fact $L_{in}^{D}\big(d'^{n}(j)\big) = L_{out}^{E}\big(d'^{n}(j)\big)$, a posteriori LLR output of the repetition decoder can be computed as

$$\Lambda_{out}^{D}\big(b^{n}(i)\big) = \sum_{j\in\chi_i} L_{in}^{D}\big(d'^{n}(j)\big), \tag{3.24}$$

the extrinsic LLR for the chip $d'^{n}(j)$ associated with $b^{n}(i)$ is given by

$$L_{out}^{D}\big(d'^{n}(j)\big) = \Lambda_{out}^{D}\big(b^{n}(i)\big) - L_{in}^{D}\big(d'^{n}(j)\big).$$

Next they are interleaved to

$$L_{in}^{E}\big(d^{n}(i)\big) = L_{out}^{D}\big(d^{n}(i)\big) = \Pi\Big(L_{out}^{D}\big(d'^{n}(i)\big)\Big).$$

Then these extrinsic information are fed to the SISO MMSE equalizer. These extrinsic information are also used by the IBI estimator. To compute IBI error expected values of the chip positions are required and are calculated by

$$\bar{d^n}(i) = tanh\left(\frac{L_{in}^E\big(d^n(i)\big)}{2}\right).$$

Next they are fed to the IBI estimation block together with the estimated channel coefficients provided by the channel estimation block. At the last iteration, decoder also computes the hard estimate $\hat{b}^n(i)$ of the transmitted information bit $b^n(i)$ by using a posteriori LLR of the given in (3.24) as

$$\hat{b}^n(i) = tanh\left(\frac{\Lambda_{out}^D\big(b^n(i)\big)}{2}\right). \tag{3.25}$$

3.4. Iterative Inter Block Interference Error Cancellation

In this section we explain how to cancel the IBI error caused by the short CP. As it is previously explained in this thesis we try to iteratively cancel out the IBI error. The proposed receiver structure is shown Figure 3.1. There we observe that the receiver is composed of different blocks each performing different tasks. These blocks are SISO FD MMSE equalizer that is for ISI cancelation, SISO repetition decoder for decoding of the received signal and IBI cancelation block that is for the estimation of the IBI error. For the data transmission a received signal block is first processed by SISO FD MMSE equalizer. The equalizer produces soft outputs. Next these outputs are fed to the repetition decoder. The decoder produces extrinsic information for each chip position as explained in previous sections. These extrinsic information are then provided to SISO FD MMSE equalizer and IBI estimator. For the channel estimation a certain number of pilot blocks are transmitted as explained in the first section of this chapter. Then these estimates are used by the equalizer and IBI estimation block during the transmission of data blocks.

Following we explain how we calculate IBI error in IBI error canceler block . The

amount of IBI error is given as

$$e^n(i) = \sum_{r=N_k+i}^{L-1} h(r)\Big\{d^{n-1}\big(N_bN_f + N_k - 1 + i - r\big) - d^n\big(N_bN_f - r + i\big)\Big\}. \qquad (3.26)$$

Here we observe that error expression is composed of three parameters these are the channel coefficient, previously and currently transmitted blocks. While we are calculating the IBI error for channel estimation we assumed that the previously and currently transmitted blocks are know, the only unknown was the channel coefficients. However, during the transmission of the information data the estimation of the IBI error is different than the estimation explained in the first section of this chapter. It is because, previously and currently transmitted data blocks are not known. Depending upon the assumption about the channel knowledge perfect channel condition or estimated channel coefficients, IBI error estimation can be done in two ways.

First way is that, channel is assumed to be known on receiver side perfectly. With this assumption remaining unknown parameters are the currently and previously transmitted data block. For the estimation of the IBI error, estimated values of the previously and currently transmitted data blocks are used which are obtained from the previous iterations.

Second way is that, we assume that the channel is not known and channel estimates are obtained with RLS channel estimation block by using training blocks. Again for the estimation of the IBI error, estimates of the transmitted data blocks that are obtained from the decoder are used.

If we assume that channel is not known, then the required channel coefficients $\hat{h}(r)$ for the estimation of IBI error term are obtained by using the RLS channel estimation algorithm. Remaining unknown parameters are previously d^{n-1} and currently d^n transmitted blocks. At that stage, we assume that several training blocks are used for the channel estimation. After the transmission of the training blocks data blocks are transmitted. The last training block is known by the receiver and it is the previously

transmitted block for the first data block. Using this fact, the only remaining unknown parameter for the calculation of the IBI error is the 1st data block which is also the currently transmitted data block. For the estimation of the IBI error of the 1st data block the estimated chip values which are obtained from the decoder are used

$$\hat{d}^n(i) = tanh\left(\frac{L_{out}^D\big(d^n(i)\big)}{2}\right)$$

The received data block is processed several times iteratively. In each iteration estimated chip values are used for the calculation of the IBI error. This calculated IBI error is subtracted from the received vector as shown in Figure 3.1 and next iteration is performed. After completing the iterations for the first block the estimated chip values of the first block are used as estimated chip values of the perviously transmitted data block for the second data block. The whole process is repeated for the second block. The IBI error term is estimated in every iteration. Thus for the mth iteration of the nth received data block we can express estimated IBI error as

$$\hat{e}_m^n(i) = a^n(i) \sum_{r=N_k+i}^{L-1} \hat{h}(r)\Big\{\hat{d}_M^{n-1}\big(N_bN_f + N_k - 1 + i - r\big) - \hat{d}_m^n\big(N_bN_f - r + i\big)\Big\}. \quad (3.27)$$

where M represents the Mth estimate of the previously transmitted data blocks. Here it is assumed that every block is processed M times. The term M can be seen as a stopping criterion for the iterative structure and the selection of the term M is very crucial in terms of complexity performance trade-off. During the simulation it is observed that, the proposed receiver structure obtains its best performance only after three iterations.

In this model after the reception of several data blocks accuracy of the IBI error estimation may decrease because of the incorrect estimates of the received data blocks. To prevent this error propagation a training block is transmitted after a certain number of data bits transmission.

3.5. Complexity Analysis

In this section, we investigate the computational complexity of the proposed receiver and make comparison between TD and FD receiver structures. On the receiver side, the channel estimator and the equalizer are the receiver components that cause most of the computational complexity. Here we consider the channel estimation and equalization separately. In the proposed receiver for channel estimation FD RLS algorithm is preferred because of its fast convergence rate, however any other algorithm would be preferred such as FD LMS with lower complexity and slower convergence rate. The amount of real multiplications and real additions required for one iteration of FD RLS and FD LMS channel estimation algorithm are given in [47]. It is reported in [49] that FD RLS algorithm is more complexity efficient, especially for long channel such as UWB channel models including approximately 400 taps, with respect to TD RLS algorithm which requires a huge matrix inversion in every iteration. For this reason, we made comparison between two different FD algorithms namely FD RLS and FD LMS algorithms.

Table 3.3. The computational complexity of FD RLS algorithm with the proposed IBI cancellation scheme

Approach	FD RLS + IBI Estimation and Cancellation
Real products	$n_s(4Mlog_2M + 22M) + n_s(2Mlog_2M + M)$
Real additions	$n_s(4Mlog_2M + 15M) + n_s(2Mlog_2M + 4M - 1)$

Table 3.4. The computational complexity of FD LMS algorithm with the proposed IBI cancellation scheme

Approach	FD LMS + IBI Estimation and Cancellation
Real products	$n_s(4Mlog_2M + 14M) + n_s(2Mlog_2M + M)$
Real additions	$n_s(4Mlog_2M + 13M) + n_s(2Mlog_2M + 4M - 1)$

Table 3.3 shows the computational complexity analysis for the proposed FD RLS algorithm, for n_s iterations, including IBI error estimation and cancellation where $M = N_b N_f$ is block length. Similarly, Table 3.4 shows the computational complexity

analysis for the FD LMS algorithm, for n_s iterations, including IBI error estimation and cancellation. For the complexity calculation it is assumed that FFT and IFFT requires roughly $2Mlog_2M$ real multiplications and additions. As seen in Table 3.3 and 3.4 , FD LMS algorithm has lower complexity than that of FD RLS algorithm, however the disadvantage is that it has slower convergence rate. In time domain receiver structures

Table 3.5. The computational complexity of the TD MMSE and the FD MMSE equalization algorithms

Approach	TD MMSE	FD MMSE
Real products	$n_s N_b(16N^2 + 4L^2 + 10L - 4N - 4)$	$n_s(4Mlog_2M + 8M)$
Real additions	$n_s N_b(8N^2 + 2L^2 + 2L - 10N + 4)$	$n_s(4Mlog_2M + 2M)$

most of the computational load is caused by the equalization stage. For this reason to decrease the computational load of the equalization stage we use FD MMSE equalizer proposed in [46] instead of TD MMSE equalizer or any other TD equalizer. The computational complexities of TD and FD MMSE equalizers to equalize N_b bits with n_s iterations are shown in Table 3.5 where N is the finite impulse response (FIR) filter that is used in TD equalizer. Usually, to obtain better performance N is chosen to be the same length with the CIR. For this reason, TD MMSE equalization in UWB systems have higher computational complexity compared to that of FD MMSE equalization as seen in Table 3.5.

4. SIMULATION RESULTS

In this chapter simulation results for the proposed receiver structure are presented. The simulations are performed by using UWB channel models CM1-CM4 proposed in [33]. In order to interleave the data blocks random interleaver is used. Pulse and chip durations are set equal to 1ns, i.e. $T_p = T_f = T_c = 1ns$. Each transmitted block is composed of 160 information bits. Each information bit is spread over 4 chips, i.e. to transmit an information bit 4 pulse with 1ns. duration is used. With this set up each block consists of 640 chips (pulse). On the receiver side matched filter outputs are sampled with sampling rate of 1ns. Thus each received block has 640 samples.The simulations are performed over 1000 different channel realizations. In order to show the effect of different channel models, the proposed receiver is simulated with CM1,CM2,CM3 and CM4 channel models.

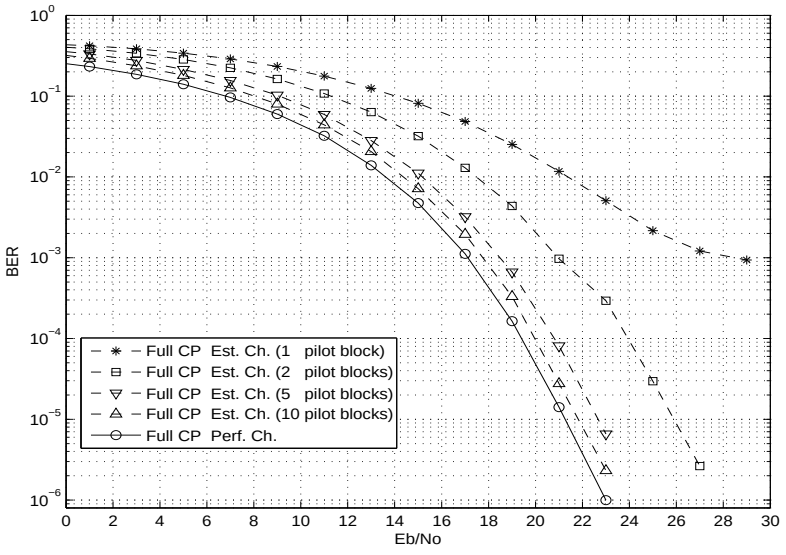

Figure 4.1. Performance of the proposed system for different number pilot blocks without IBI cancellation CM4 channel

As indicated in previous chapter, both FD MMSE equalizer and the IBI error estimator uses estimated channel coefficients. That is why, the receiver's BER performance is highly affected by the channel estimator's performance. As indicated in

Figure 3.3, channel estimation performance increases with pilot block number. To see the effect of the channel estimation performance on the receiver's BER performance, we simulated the proposed receiver when full CP is employed over CM4 with different number of pilot blocks used for channel estimation assuming perfect state information is available on the receiver side. Results are shown in Figure 4.1. Since full CP is employed, there is no IBI error. It is observed that, the receiver's performance increases with the increased pilot block number as expected. While there is a huge performance improvement between 1 pilot block and 2 pilot blocks cases, there is only a small amount of performance gain between 5 and 10 pilot blocks cases. Moreover, there is only 0.8 dB performance difference at 10^{-5} BER between perfect channel estimation case and channel estimation with 10 pilot blocks case. Considering these results, there is no need to use more than 10 pilot blocks if one is satisfied with 0.8 dB performance lost at 10^{-5} BER.

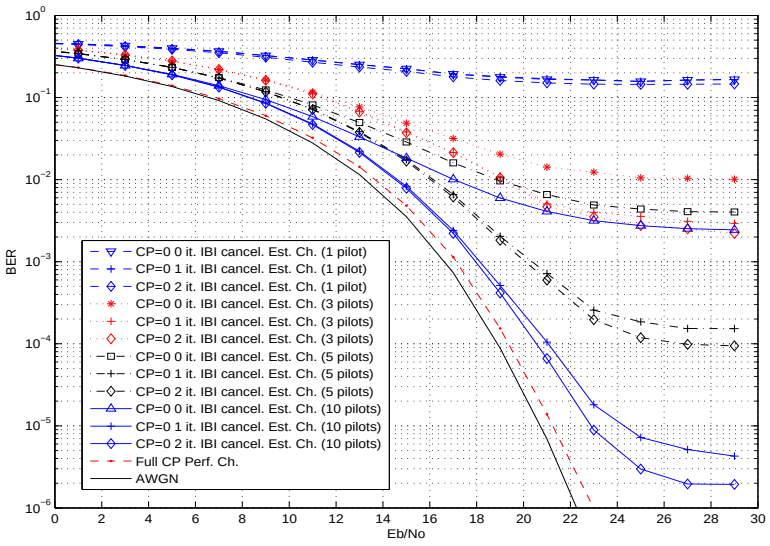

Figure 4.2. Performance comparison of the proposed system with different number pilot blocks for CP=0 with IBI cancellation CM4 channel

In order to see the effect of short CP usage on the proposed receiver structure, we simulated the our system over different UWB channel model with different CP lengths. Figure 4.2 and 4.3 shows the performance of the proposed receiver for CM4 channel when CP length is set to be zero and 20 respectively and when IBI cancellation is

applied. In agreement with results obtained in Figure 4.1, increasing the number of pilot blocks causes improvement on the detection performance in both Figure 4.2 and 4.3. As expected, the BER performance of the proposed receiver, with short CP and when no inter block interference is applied, is worse compared to results obtained for full CP case indicated in Figure 4.1 independent of the number of pilot blocks used for channel estimation.

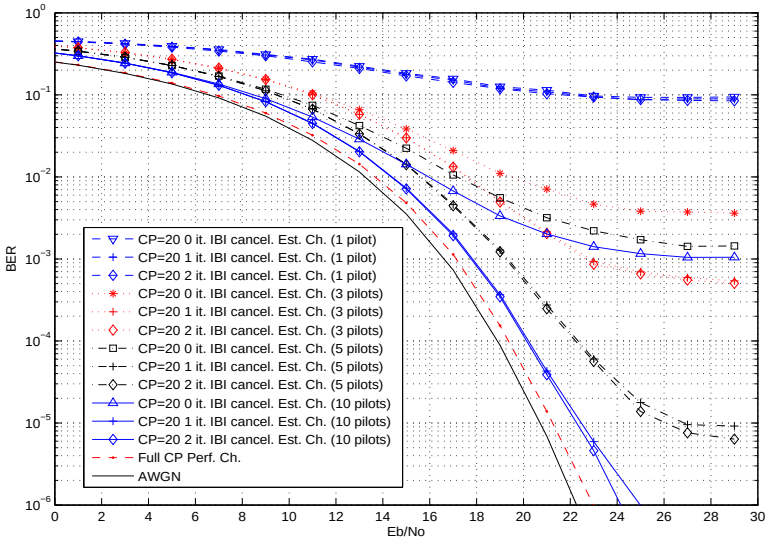

Figure 4.3. Performance comparison of the proposed system with different number pilot blocks for CP=20 with IBI cancellation CM4 channel

It is also observed that applying IBI error cancellation improves the receiver performance over iterations. However, the amount of improvement is highly affected by the initial performance of the receiver, i.e., when no IBI cancelation is applied. In addition to initial data estimates, another parameter that is affecting the effectiveness of the proposed IBI cancellation scheme is the number of pilot blocks used for channel estimation. The effect of these two can be seen from the upper three BER curves on both Figure 4.2 and 4.3 corresponding to no IBI cancellation, IBI cancellation with one and three iterations respectively. Here, because of the previously mentioned reasons, only a small amount of performance improvement is obtained by proposed IBI cancellation scheme. However, when the pilot block number is increased much more performance gain is obtained. For example, in Figure 4.2, when 10 pilot blocks

are used and after three iterations there is approximately 1.5 dB difference between proposed IBI cancellation scheme and AWGN performance of the proposed receiver at 10^{-4} BER.

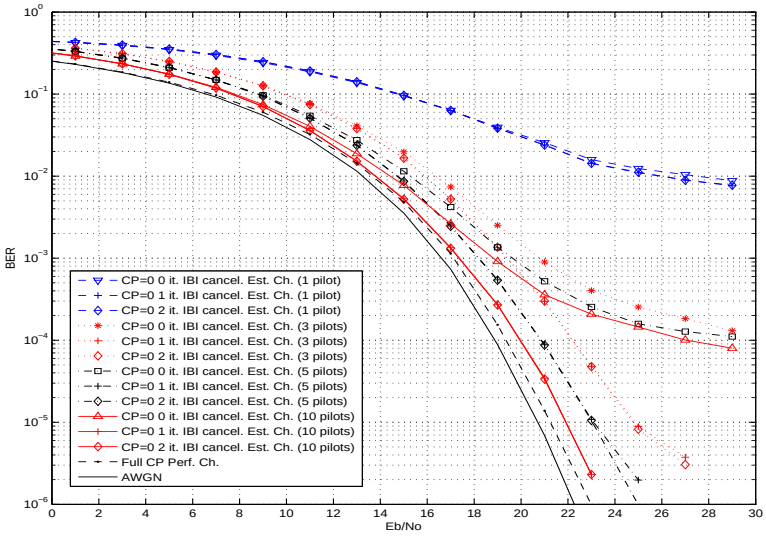

Figure 4.4. Performance comparison of the proposed system with different number pilot blocks for CP=0 with IBI cancellation CM1 channel

Up to now, only CM4 channel model, which is a NLOS channel with 360 taps, is considered for simulations. To see the performance of the proposed receiver structure on CM1 channel model which is a LOS channel with 114 taps, we performed the simulations with same setup that is used for Figures 4.2-4.3, that is CP length is set to be zero and 20, while four different number of pilot blocks are used for channel estimation. The results are shown in Figures 4.4-4.5. Comparing simulation results obtained for CM1 and CM4, it is observed that the proposed receiver structure performs better for CM1 as expected. For example, comparing the first line of Figures 4.2-4.4 corresponding to zero CP case with 1 pilot block channel estimation, it is evident that while for CM4 saturation is obtained around 10^{-1} for CM1 saturation is obtained at 10^{-2}. Figure 4.6 shows the performance of the proposed receiver without IBI cancellation for all different channel models. Cyclic prefix length is set to be zero and channel estimation is done by using 5 pilot blocks.

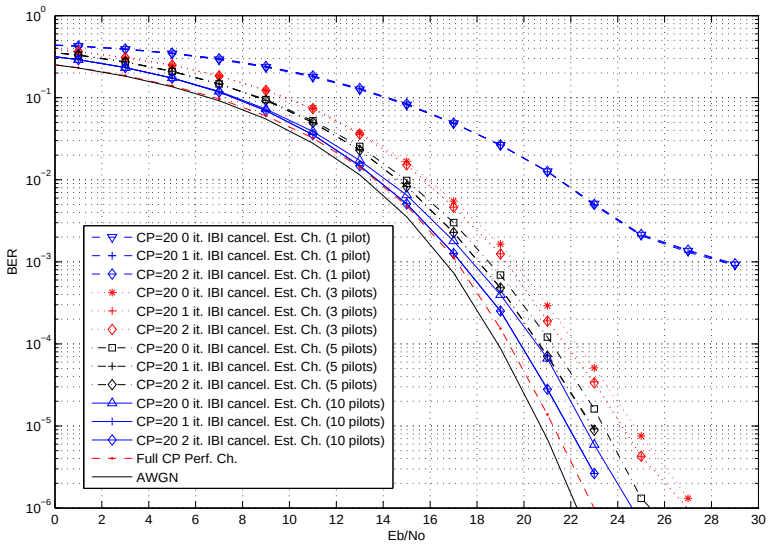

Figure 4.5. Performance comparison of the proposed system with different number pilot blocks for CP=20 with IBI cancellation CM1 channel

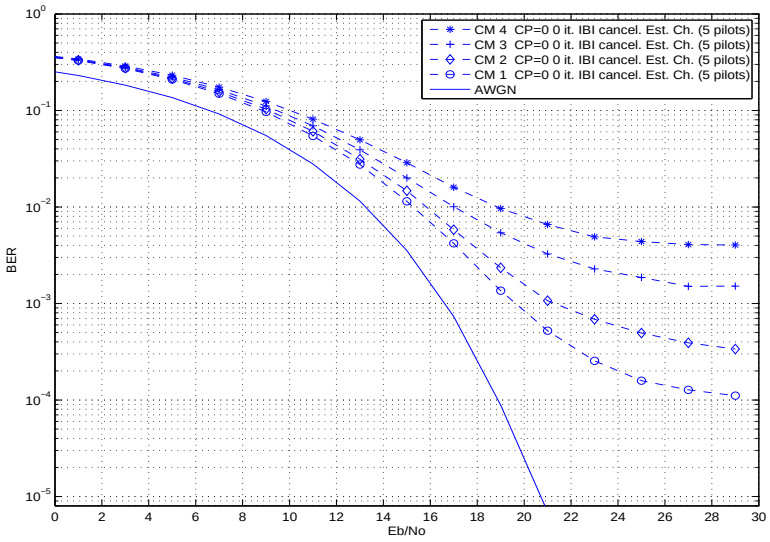

Figure 4.6. Performance of the proposed receiver over different channel models without IBI cancellation CP=0 channel estimation with 5 pilot blocks

As we expected, the proposed receiver performs worst for CM4 channel which is a NLOS channel with an extreme delay profile. Consistently, the best performance is

obtained for CM1 channel which has lower delay profile compared to CM4 channel. In Figure 4.7 simulation results over different channel models for the proposed receiver with iterative IBI cancelation is depicted.

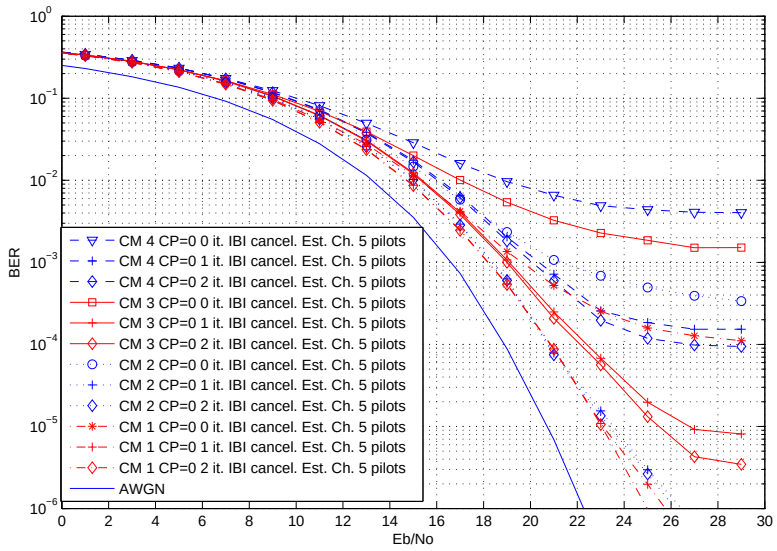

Figure 4.7. Performance of the proposed receiver over different channel models with IBI cancellation CP=0 channel estimation with 5 pilot blocks

It is observed that the proposed IBI scheme causes substantial increase in the receiver performance for all channel models. The greatest performance is improvement is obtained for CM1 channel model. It is because, the initial performance of the receiver for CM1 is better than that of other channel models. Thus the IBI error estimation is more accurate. During the simulations it is observed that most of the performance improvement is obtained with the first iteration. After the first iteration small amount of improvement is obtained over subsequent iterations, which is common for this kind of iterative algorithms. That is at some point algorithm saturates and does not provide any performance improvement over iterations.

5. CONCLUSIONS

In this thesis, we considered FD reception of IR-UWB signals with short CP. An iterative receiver structure is proposed to combat with the deteriorating effects caused by the short CP usage. For channel estimation, we proposed a FD RLS algorithm combined with IBI cacelattion algorithm. It is shown that the proposed algorithm improves the channel estimation performance. A similar IBI cancellation scheme is proposed for the back end of the receiver to improve the detection performance. It is also shown that substantial detection performance gain can be obtained by employing iterative IBI cancelation. Although, we obtain such performance gain, it is observed that proposed IBI cancellation scheme is highly affected by the channel estimation performance.

APPENDIX A: Derivation of the IBI Error

For better understanding of the IBI error derivation we explain how IBI error occurs when CP length is shorter than CIR. Figure A.1 illustrates a simple scenario for short CP case. There we assume channel has 7 taps while CP length is 3. It is observed that first received sample r_0^n is corrupted by last three samples $x_{N-3}^{n-1}, x_{N-2}^{n-1}, x_{N-1}^{n-1}$ of the previously transmitted block. Similarly, r_1^n is corrupted by $x_{N-2}^{n-1}, x_{N-1}^{n-1}$ and r_2^n is corrupted by x_{N-1}^{n-1}. If CP length were longer than CIR, then $x_{N-6}^n, x_{N-5}^n, x_{N-4}^n$ would be multiplied with last three CIR coefficients h_6, h_5, h_4 instead of $x_{N-3}^{n-1}, x_{N-2}^{n-1}, x_{N-1}^{n-1}$ for the calculation of the first received sample r_0^n. Thus, the IBI error for the first received sample is the difference between short CP case and full CP case and can be expressed as

$$e(0) = h_6(x_{N-3}^{n-1} - x_{N-6}^n) + h_5(x_{N-2}^{n-1} - x_{N-5}^n) + h_4(x_{N-1}^{n-1} - x_{N-4}^n). \tag{A.1}$$

Similarly, the IBI error for the second and third received samples can be calculated.

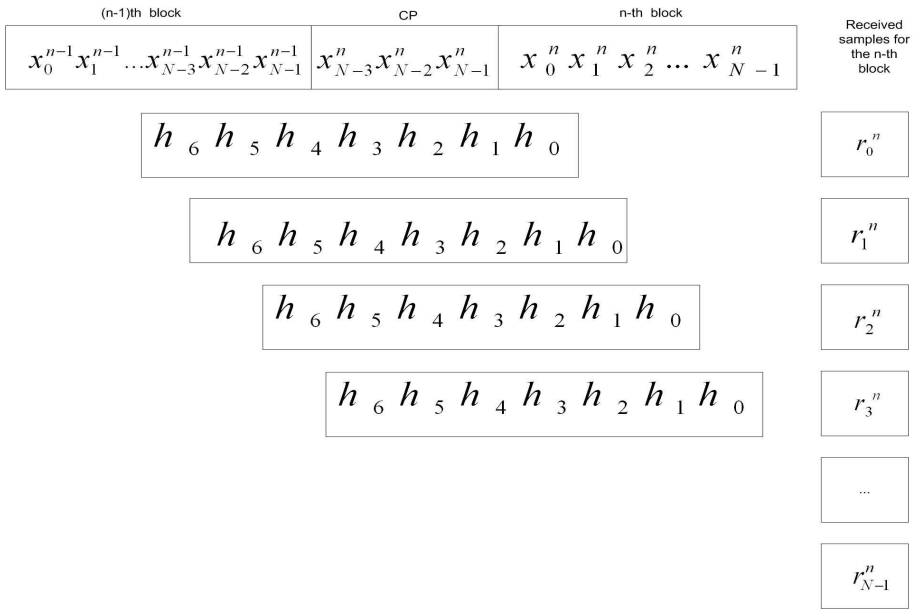

Figure A.1. IBI due to insufficient CP

Following the same methodology we can derive the IBI error $e^n(i)$ for general case where CIR length and CP length can be variable. The derivation is as following. We assume that each transmitted data block is composed of N_bN_f chips and it is equal or greater then channel impulse response $N_bN_f \geq L$. Thus when CP length is shorter than the CIR or even in the absence of a CP IBI error present in nth data samples are limited to be caused only from (n-1)th data block. Keeping these in minds we define a term $\triangle = L - N_k$ representing the difference between the channel impulse response and CP. Thus nth and (n-1)th transmitted data blocks are

$$\begin{aligned}
&\ldots d^{n-1}(N_bN_f - \triangle)d^{n-1}(N_bN_f - \triangle + 1)d^{n-1}(N_bN_f - \triangle + 2)d^{n-1}(N_bN_f - \triangle + 3) \\
&\ldots d^{n-1}(N_bN_f - 4)d^{n-1}(N_bN_f - 3)d^{n-1}(N_bN_f - 2)d^{n-1}(N_bN_f - 1) \\
&d^n(N_bN_f - N_k)d^n(N_bN_f - N_k + 1)d^n(N_bN_f - N_k + 2)d^n(N_bN_f - N_k + 3)\ldots \\
&\ldots d^n(N_bN_f - 4)d^n(N_bN_f - 3)d^n(N_bN_f - 2)d^n(N_bN_f - 1)d^n(0)d^n(1)d^n(2)d^n(3)d^n(4)\ldots \\
&\ldots d^n(\triangle - 2)d^n(\triangle - 1)d^n(\triangle)\ldots d^n(N_bN_f - 4)d^n(N_bN_f - 3)d^n(N_bN_f - 2)d^n(N_bN_f - 1)
\end{aligned} \tag{A.2}$$

First element of the nth received block that contains IBI error $r^n_{IBI}(0)$ is obtained by convolving the CIR and transmitted data block.

$$\begin{aligned}
r^n_{IBI}(0) = {} & d^n(0)h(0) + d^n(N_bN_f - 1)h(1) + d^n(N_bN_f - 2)h(2) + d^n(N_bN_f - 3)h(3)\ldots \\
& \cdots + d^n(N_bN_f - N_k + 3)h(L - \triangle - 4) + d^n(N_bN_f - N_k + 2)h(L - \triangle - 3) + \\
& + d^n(N_bN_f - N_k + 1)h(L - \triangle - 2) + d^n(N_bN_f - N_k)h(L - \triangle - 1) + \\
& + d^{n-1}(N_bN_f - 1)h(L - \triangle) + d^{n-1}(N_bN_f - 2)h(L - \triangle + 1) + \\
& + d^{n-1}(N_bN_f - 3)h(L - \triangle + 2) + d^{n-1}(N_bN_f - 4)h(L - \triangle + 3)\ldots \\
& + d^{n-1}(N_bN_f - \triangle + 3)h(L - 4) + d^{n-1}(N_bN_f - \triangle + 2)h(L - 3) + \\
& + d^{n-1}(N_bN_f - \triangle + 1)h(L - 2) + d^{n-1}(N_bN_f - \triangle)h(L - 1).
\end{aligned} \tag{A.3}$$

If the CP length were sufficient then the first term of the nth received block $r^n(0)$

would be

$$
\begin{aligned}
r^n(0) = {} & d^n(0)h(0) + d^n(N_bN_f - 1)h(1) + d^n(N_bN_f - 2)h(2) + d^n(N_bN_f - 3)h(3)\,..(A.4)\\
& \cdots + d^n(N_bN_f - L + \triangle)h(L - \triangle) + d^n(N_bN_f - L + \triangle - 1)h(L - \triangle + 1)\ldots\\
& + d^n(N_bN_f - L + 3)h(L - 3) + d^n(N_bN_f - L + 2)h(L - 2) +\\
& + d^n(N_bN_f - L + 1)h(L - 1).
\end{aligned}
$$

Then IBI error contained in the first element of the received vector is $e^n(0) = r^n_{IBI}(0) - r^n(0)$ where $e^n(0)$ is expressed as

$$
\begin{aligned}
e^n(0) = {} & \Big(d^{n-1}(N_bN_f - 1) - d^n(N_bN_f - L + \triangle)\Big)h(L - \triangle) + \qquad (A.5)\\
& + \Big(d^{n-1}(N_bN_f - 2) - d^n(N_bN_f - L + \triangle - 1)\Big)h(L - \triangle + 1) +\\
& + \Big(d^{n-1}(N_bN_f - 3) - d^n(N_bN_f - L + \triangle - 2)\Big)h(L - \triangle + 2)\ldots\\
& + \Big(d^{n-1}(N_bN_f - \triangle + 2) - d^n(N_bN_f - L + 3)\Big)h(L - 3) +\\
& + \Big(d^{n-1}(N_bN_f - \triangle + 1) - d^n(N_bN_f - L + 2)\Big)h(L - 2) +\\
& + \Big(d^{n-1}(N_bN_f - \triangle) - d^n(N_bN_f - L + 1)\Big)h(L - 1).
\end{aligned}
$$

Similarly IBI error term for $e^n(1)$ is

$$
\begin{aligned}
e^n(1) = {} & \Big(d^{n-1}(N_bN_f - 1) - d^n(N_bN_f - L + \triangle)\Big)h(L - \triangle + 1) + \qquad (A.6)\\
& + \Big(d^{n-1}(N_bN_f - 2) - d^n(N_bN_f - L + \triangle - 1)\Big)h(L - \triangle + 2) +\\
& + \Big(d^{n-1}(N_bN_f - 3) - d^n(N_bN_f - L + \triangle - 2)\Big)h(L - \triangle + 3)\ldots\\
& + \Big(d^{n-1}(N_bN_f - \triangle + 2) - d^n(N_bN_f - L + 3)\Big)h(L - 2) +\\
& + \Big(d^{n-1}(N_bN_f - \triangle + 1) - d^n(N_bN_f - L + 2)\Big)h(L - 1).
\end{aligned}
$$

and for the $(\triangle - 1)$th elemenet of the nth received vector IBI error $e^n(\triangle - 1)$ is

$$e^n(\triangle - 1) = \Big(d^{n-1}(N_b N_f - 1) - d^n(N_b N_f - L + \triangle)\Big)h(L-1). \tag{A.7}$$

Closed form of the IBI error is

$$e^n(i) = \sum_{r=L-\triangle+i}^{L-1} h(r)\Big(d^{n-1}(N_b N_f + L - \triangle - 1 + i - r) - d^n(N_b N_f - r + i)\Big). \tag{A.8}$$

Final expression for IBI error is obtained by replacing $\triangle$ with $\triangle = L - N_k$ in equation A.7

$$e^n(i) = \sum_{r=N_k+i}^{L-1} h(r)\Big\{d^{n-1}\big(N_b N_f + N_k - 1 + i - r\big) - d^n\big(N_b N_f - r + i\big)\Big\}. \tag{A.9}$$

REFERENCES

1. V. Erceg *et al.*, "A model for the multipath delay profile of fixed wireless channels," *IEEE JSAC.*, Vol. 17, No. 3, pp. 399-410, Mar. 1999.

2. J. A. C. Bringham, "Multicarrier modulation for data transmission: An idea whose time has come," *IEEE Commun. Mag.*, Vol. 28, No. 5, pp. 5-14, May 1990.

3. L. J. Cimini, "Analysis and simulation of a digital mobile channel using orthogonal frequency division multiplexing," *IEEE Trans Commun.*, Vol. 33, No. 7, pp. 665-675, July 1985.

4. J. T. E. McDonell and T.A. Wilkinson,"Comparison of computational complexity of adaptive equalization and OFDM for indoor wireless networks," *Proc. PIMRC'96*, Taipei, Taivan, pp. 1088-1090.

5. H. Zou et al, "Equilezed GMSK, equalized QPSK and OFDM, a cmperative study for high-speed wireless indoor data communications," *VTS'99*, Spring, Houston, USA, May 1999.

6. U. Dettmar et al, " Modulation for HIPERLAN type 2," *VTS'99*, Spring, Houston, USA, May 1999.

7. J. G. Proakis, *Digital Communications*, 3th ed. McGraw-Hill 1995.

8. S. U. H. Qureshi, "Adaptive equalization," *Proc. IEEE*, Vol. 73, pp. 1349-1387, 1985.

9. S. Ariyavisitakul and L. J. Greenstein, "Reduced-complexity equalization for broadband wireless chammels," *IEEE J. Selec. Areas Commun.*, Vol. 15, pp. 5-15, Jan 1997.

10. T. Walzman and M. Schwartz, "Automatic equalizaiton using the discrete fre-

quency domain," *IEEE Trans. Inform. Theory*, Vol. IT-19, pp. 59-68, 1973.

11. D. Maiwald, H. P. Kaesar and F. Closs, "An adaptive equalizer with significantly reduced number of operations," *in Proc. IEEE Int. Conf. Acoustics, Speech, Signal Processing (ICASSP)*, pp. 100-104, Apr. 1978.

12. J. J. Shynk, "Frequency-domain and multirate adaptive filtering," *IEEE Signal Processing Mag.*,pp. 14-35, 1992.

13. H. Sarı, G. Karam and I. Jeanclaude, "Frequency-domain equalization of mobile radio and terrestrial broadcast channels," *Proc. GLOBECOM'94*,San Francisco, CA, Nov.-Dec. 1994, pp 1-5

14. H. Sarı, G. Karam and I. Jeanclaude, "Transmission techniques for digital terrestrial TV broadcasting," *IEEE Commun. Mag.*, Vol. 33, No. 2, pp. 100-109, Feb. 1995.

15. H. Sarı, G. Karam and I. Jeanclaude, "Analysis of orthogonal frequency-division multiplexing for mobile radio applications," *VTC'94 Conf. Rec.*, Vol. 3, June 1994, Stockholm, pp. 1635-1639.

16. D. Falconer, S. Ariyavisitakul, A. Benyamin-Seeyar and B. Eidson, "Frequency domain equalization for single-carrier broadband wireless systems," *IEEE Commun. Mag.*, Vol. 40, no. 4, pp. 58-66, Apr. 2002.

17. A. Czyliwk, "Comparison between adaptive OFDM and single carrier modulation with frequency domain equalization," *VTC'96 Conf. Rec.*, Phoenix, AZ, Vol. 21, No. 2, pp. 865-869, May 1997.

18. P. J. W. Melisa, R. C. Younce and C. E. Rohrs, "Impule responce shortening for discrete multitone transceivers," *IEEE Trans. Commun.*, Vol. 44, No. 12, pp. 1662-1672, 1996.

19. T. Hwang and Y. Li, "Iterative cyclic prefix reconstruction for coded single-carrer

systems with frequency-domain equalization (SC-FDE)," *Proc. IEEE Veh. Technol. Conf.*, Vol. 3, pp. 1841-1845, Apr. 2003.

20. A. Gustamo, P. Torres, R. Dinis and N. Esteves, "A Reduced-CP approach to SC/FDE block transmission for broadband wireless communications," *IEEE Trans. Commun.*, Vol. 55, no. 4, pp. 801-809, Apr. 2007.

21. A. Gustamo, P. Torres, R. Dinis and N. Esteves, "A class of iterative FDE echniques for reduced-CP SC-based block transmission," *Proc. IEEE 4th Int. Symp. Turbo Codes, Related Topics*, Apr. 2006, Paper 71, Session 13.

22. K. Hayashi and H. Sakai, "Interference cancellation schemes for single-carrier block transmission with insufficient cyclic prefix," *EURASIP Journal on Wireless Communications and Networking*, vol. 2008, no. 1, Jan. 2008.

23. L. Yang and G. B. Giannakis, "Ultra wideband communications: An idea whose time has come," *IEEE Signal Process. Mag.*, Vol. 21, No. 6, pp. 26-54, Nov. 2004.

24. First Report and Order in Matter of revision of Part 15 of the Commission's Rules Regarding Ultra-Wideband Trasmission Systems. ET Docket 98-153, Federal Communication Commission, FCC 02-48, April 22, 2002.

25. M. Z. Win and R. A. Scholtz, "Impulse radio: How it works," *IEEE Commun. Letters.*, Vol. 2, No. 2, pp. 36-38, Feb. 1998.

26. M. Z. Win and R. A. Scholtz, "Ultra-wide bandwidth time-hopping spread-spectrum impulse radio for wireless multiple-access communicatins ," *IEEE Trans. Commun.*, Vol. 48, No. 4, pp. 679-691, Apr. 2000.

27. B. M. Sadler and A. Swami, "On the performance of UWB and DS-spread spectrum communication systems," *IEEE Conf. on Ultra Wideband Syst. and Technologies*, pp. 289-292, 2002.

28. F. Ramirez-Mireles, "Performance of ultrawideband SSMA using time hopping and

M-ary PPM," *IEEE Jour. Selec. Areas in Commun.*, Vol. 19, No. 6, pp. 1186-1196, June 2001.

29. N. Boubaker and K. B. Letaief, "Ultra wideband DSSS for multiple access communication using antipodal signaling," *IEEE Int. Conf. on Commun. 2003*, Vol. 3, pp. 2197-2201, 11-15 May 2003.

30. G. R. Aiello and G. D. Rogerson, "Ultra-wideband wireless systems," *IEEE Microwave Mag.*, Vol. 4, no. 2, pp. 36-47, June 2003.

31. A. Rajeswaran, V. S. Somayazulu and J. R. Foerster, "Rake performance for a pulse based UWB system in a realistic UWB indoor channel," *IEEE Int. Conf. on Commun., 2003*, Vol. 4, pp. 2879-2883, 11-15 May 2003.

32. M. Z. Win and R. A. Scholtz, "Characterization of ultra-wide bandwidth wireless indoor channels: a communication-theoretic view," *IEEE Jour. Selected Areas Commun.*, Vol. 20, No. 9, pp. 1613-1627, Dec. 2002.

33. J. R. Foerster,"Channel modeling sub-committee repot (final)," Tech. Rep. P802.15-02/368r5-SG3a, IEEE P802.15 Working Group for Wireless Personal Area Networks (WPANs), Dec. 2002.

34. Y. Ishiyama and T. Ohtsuki, "Performance evaluation of UWB-IR and DS-UWB with MMSE-frequency domain equalization," *IEEE Global Telecommunication Conf., 2004*, Vol. 5,pp. 3093-3097, 29 Nov.-3Dec. 2004.

35. Y. Wang, X. Dong, P. H. Wittke and S. Mo, "Cyclic prefixed single carrier transmission in ultra-wideband communications," *IEEE Tans. on Wireless Commun.*, Vol. 5, No. 8, pp. 2017-2021, August 2006.

36. P. Kaligineedi and V. K. Bhargava, "Frequency-domain equalization techniques for DS-UWB systems," *IEEE Glob. Telecommun. Conf., 2006*, pp. 1-6, Nov. 2006.

37. Sujin Kim, Keonkook Lee, Jongsub Cha, Joonhyuk Kang, Naesoo Kim and

Sangjoon Park, "Frequency domain equalizer using zero padding for IR-UWB systems," *IEEE Int. Conf. on Ultra-Wideband, 2007*, pp. 905-909, 24-26 Sept. 2007.

38. S. Yoshida and T. Ohtsuki, "Improvement of bandwidth efficiency of UWB-IR and DS-UWB with frequency-domain equalization (FDE) based on Cyclic Prefix Reconstruction," *Proc. of VTC*, Vol. 2, pp. 25-28, Sept. 2005.

39. S. Yoshida and T. Ohtsuki, "Effect of imperfect channel estiamtion on the performance of UWB-IR with frequency-domain equalization (FDE) and cyclic prefix reconstruction," *IEIC Technical Report(Institute of Electronics, Information and Communication Engineers)*, Vol. 105, no. 620, pp. 5-10, 2006.

40. K. Takeda, H. Tomeba and F. Adachi, "Iterative overlap FDE for DS-CDMA without GI," *IEEE Procc. of Veh. Tech. Conf., VTC'06*, Montreal, Quebec, Canada, pp. 2038-2042, Sept. 2006.

41. Y. Li, S. McLaughlin and D. G. M. Cruickshank, "Bandwidth efficient single carrier systms with frequency domain equalization," *Electron. Lett.*, Vol. 41, No. 15, pp. 857-858, July 2005.

42. H. Liu and P. Schniter, "Iterative frequency-domain channel estimation and equalization for single-carrier transmission without cyclic-prefix," *IEEE Trans. on Wireless Commun.*, Vol. 7, No. 10, pp. 3686-3691, October 2008.

43. W. Koch and A. Baier, "Optimum and sub-optimum detection of coded data disturbed by time varying intersymbol interference" *IEEE Proceedings on the Global Telecommunications Conference '90* December 1990, pp. 1679-1684.

44. X. Wang and H. V. Poor, "Turbo multiuser detection and equalization for coded CDMA in multipath channels," *IEEE International Conference on Universal Personal Comunications*, Vol. 2, pp. 3686-3691, 1998.

45. M. Tuchler, R. Koetter, and A. Singer "Turbo equalization: Principles and new

results," *IEEE Transactions on Communications* , Vol. 50, pp. 754-767, May 2002.

46. M. Tuchler and J. Hagenauer, "Turbo equalization using frequency domain equalizers," *Proc. of the Allerton Conference, Monticello, IL, U.S.A.*, October 2000.

47. M. Morelli, L. Sanguinetti, and U. Mengali, "Channel estimation for adaptive frequency-domain equalization," *IEEE Trans. on Wireless Commun.*, vol. 4, No. 5, pp. 2508-2518, Sep. 2005.

48. K. Li, X. Wang, G. Yue, and L. Ping, "A low rate code-spread and chip-interleaved time-hopping UWB system," *IEEE J. Select. Area. Comm.*, vol. 24, no. 4, pp. 864-870, April 2006.

49. E. Ersen, "Synchronization, channel estimation and detection for ultra-wideband systems," Master's thesis, Bogazici University, Turkey, 2006